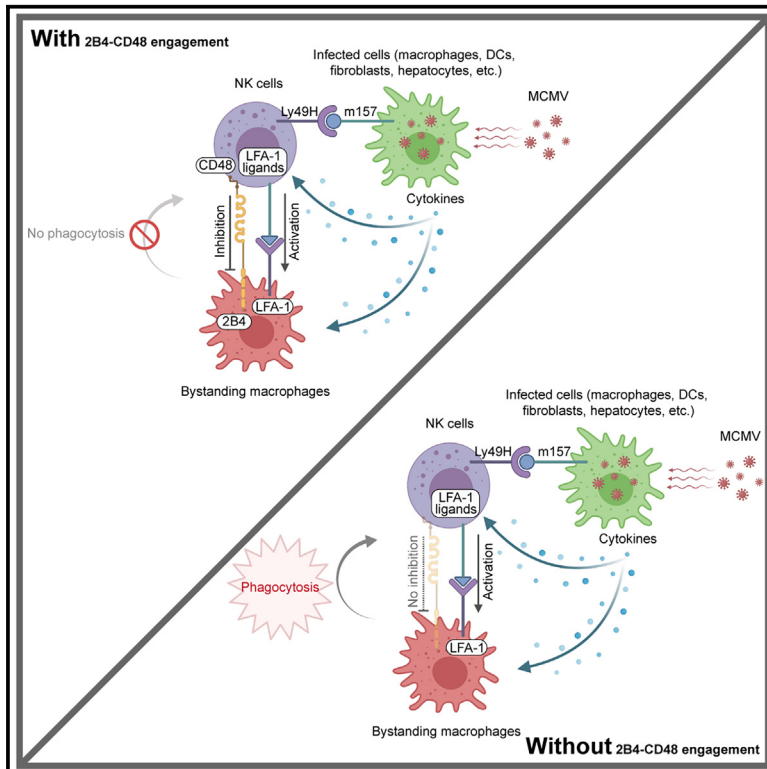


Suppression of adaptive NK cell expansion by macrophage-mediated phagocytosis inhibited by 2B4-CD48

Graphical abstract



Authors

Rui Li, Cristian Camilo Galindo, Dominique Davidson, ..., Silvia M. Vidal, Joseph C. Sun, André Veillette

Correspondence

andre.veillette@ircm.qc.ca

In brief

Li et al. demonstrate that the 2B4-CD48 axis suppresses phagocytosis of adaptive NK cells by activated macrophages during MCMV infection by inhibiting the pro-phagocytic integrin LFA-1 on macrophages. This NK cell-extrinsic mechanism promotes the generation of long-lived adaptive NK cells.

Highlights

- CD48 on NK cells and 2B4 on macrophages suppress phagocytosis of NK cells in MCMV infection
- LFA-1 is the key pro-phagocytic receptor on macrophages in MCMV infection
- Bystanding macrophages, not infected ones, phagocytose activated Ly49H⁺ NK cells



Article

Suppression of adaptive NK cell expansion by macrophage-mediated phagocytosis inhibited by 2B4-CD48

Rui Li,^{1,2} Cristian Camilo Galindo,^{1,2} Dominique Davidson,¹ Huajjian Guo,^{1,2} Ming-Chao Zhong,¹ Jin Qian,¹ Bin Li,^{1,3} Zsolt Ruzsics,⁴ Colleen M. Lau,⁵ Timothy E. O'Sullivan,⁶ Silvia M. Vidal,^{7,8} Joseph C. Sun,^{9,10} and André Veillette^{1,2,3,11,*}

¹Laboratory of Molecular Oncology, Institut de Recherches Cliniques de Montréal (IRCM), Montréal, QC H2W 1R7, Canada

²Department of Medicine, McGill University, Montréal, QC H3G 1Y6, Canada

³Molecular Biology Program, University of Montréal, Montréal, QC H3T 1J4, Canada

⁴Institute of Virology, University Medical Center, Faculty of Medicine, University of Freiburg, 79104 Freiburg, Germany

⁵Microbiology and Immunology, College of Veterinary Medicine, Cornell University, Ithaca, NY 14853, USA

⁶Department of Microbiology, Immunology, and Molecular Genetics, David Geffen School of Medicine at UCLA, Los Angeles, CA 90095, USA

⁷Department of Human Genetics, McGill University, Montréal, QC H3A 0C7, Canada

⁸Dahdaleh Institute of Genomic Medicine, McGill University, Montréal, QC H3A 0G1, Canada

⁹Immunology Program, Memorial Sloan Kettering Cancer Center, New York, NY 10065, USA

¹⁰Department of Immunology and Microbial Pathogenesis, Weill Cornell Medical College, New York, NY 10065, USA

¹¹Lead contact

*Correspondence: andre.veillette@ircm.qc.ca

<https://doi.org/10.1016/j.celrep.2024.113800>

SUMMARY

Infection of mice by mouse cytomegalovirus (MCMV) triggers activation and expansion of Ly49H⁺ natural killer (NK) cells, which are virus specific and considered to be “adaptive” or “memory” NK cells. Here, we find that signaling lymphocytic activation molecule family receptors (SFRs), a group of hematopoietic cell-restricted receptors, are essential for the expansion of Ly49H⁺ NK cells after MCMV infection. This activity is largely mediated by CD48, an SFR broadly expressed on NK cells and displaying augmented expression after MCMV infection. It is also dependent on the CD48 counter-receptor, 2B4, expressed on host macrophages. The 2B4-CD48 axis promotes expansion of Ly49H⁺ NK cells by repressing their phagocytosis by virus-activated macrophages through inhibition of the pro-phagocytic integrin lymphocyte function-associated antigen-1 (LFA-1) on macrophages. These data identify key roles of macrophages and the 2B4-CD48 pathway in controlling the expansion of adaptive NK cells following MCMV infection. Stimulation of the 2B4-CD48 axis may be helpful in enhancing adaptive NK cell responses for therapeutic purposes.

INTRODUCTION

Activation of natural killer (NK) cells is controlled by a wide array of monomorphic receptors, which are triggered by ligands that may or may not be expressed on potential “target” cells, including virus-infected cells and cancer cells.^{1–3} When activating receptors are triggered predominantly over inhibitory receptors, NK cells are activated and display effector functions.^{1–3} Effector functions include cytotoxicity toward target cells, a process mediated primarily by the release of granzyme-B-containing granules, and production of pro-inflammatory cytokines such as interferon (IFN)- γ . Because of their ability to kill cancer cells, there is increasing interest in using NK cells for anti-cancer immunotherapy, in particular against hematological malignancies, which are highly sensitive to NK cell killing.^{1,4,5}

Unlike T cells and B cells, NK cells were long considered to be devoid of memory potential. However, recent studies have provided clear evidence that “adaptive” or “memory” NK cells (hereafter named adaptive NK cells) exist.^{4,6–11} So far, the exis-

tence of these cells has been confirmed in two major settings: after infection by viruses such as mouse cytomegalovirus (MCMV) and human cytomegalovirus (HCMV) and after stimulation with cytokines like IL-12 and IL-18. It is believed that virus-induced adaptive NK cells are truly antigen specific. However, cytokine-activated NK cells do not seem to be antigen specific and are often referred to as “cytokine-induced memory-like” (CIML) NK cells.

The notion that virus-specific adaptive NK cells exist was most elegantly demonstrated after MCMV infection in mice.^{8,9,11} When transferred into uninfected mice, NK cells isolated from mice previously infected with MCMV conferred stronger and specific protection against repeated MCMV infection compared with NK cells derived from non-infected mice. Virus-specific NK cells robustly expand after MCMV infection as a result of triggering of the NK cell-activating receptor Ly49H, which recognizes the MCMV-encoded protein m157 on a wide range of infected cells. Receptors responsible for the generation of adaptive NK cells in response to other viruses have not been identified.



Using the MCMV model, three phases in the expansion of adaptive NK cells have been identified: activation, proliferation, and suppression.^{9,12} These processes all take place within 7 days of infection. Until now, a limited number of signaling molecules have been found to play critical roles at each of these steps. The receptors Ly49H and DNAM-1, as well as the adaptor DAP12, are key for the initial activation and proliferation of Ly49H⁺ NK cells.^{11,13} This response occurs within 4 days post-infection. Then, the cytokines IL-12 and IL-18, in addition to their receptors and STAT effectors, amplify NK cell proliferation to generate a large pool of activated virus-specific NK cells.^{14–16} This response is limited by elimination of the majority of activated Ly49H⁺ NK cells. Although poorly understood, this suppression phase is likely complex and is prevented by type I IFN signaling, which prevents killing of activated Ly49H⁺ NK cells by other NK cells.^{17,18}

SLAM family receptors (SFRs) are a group of six canonical transmembrane receptors named SLAMF1, 2B4 (SLAMF4), SLAMF6, SLAMF7, SLAMF5 (CD84), and Ly-9 (SLAMF3).^{19–22} These receptors are expressed only on hematopoietic cells. Most SFRs are homotypic receptors (i.e., self-ligands), with the exception of 2B4, which recognizes as ligand CD48 (SLAMF2), a non-canonical SFR also expressed on hematopoietic cells. Unlike canonical SFRs, CD48 is glycosylphosphatidylinositol (GPI) linked and is devoid of a cytoplasmic domain. All six canonical SFR-encoding genes, in addition to the gene coding for CD48, are located on the same locus on chromosome 1 in humans and mice. Canonical SFRs trigger either inhibitory or activating intracellular signals, which control several key immune cell functions. However, CD48 is generally viewed as a ligand that triggers the activity of 2B4.^{19–21}

SFRs play key roles in NK cells.^{19,21,22} 2B4 is an inhibitory receptor, at least in mice, that suppresses NK cell activation in response to target cells expressing its ligand, CD48. An opposite function was described in human NK cells. In both mouse and human NK cells, SLAMF7 is an activating receptor that promotes NK cell activation in response to target cells bearing its ligand, SLAMF7. Last, SLAMF6 and 2B4 have been implicated in NK cell education, possibly as a result of their ability to trigger inhibitory signals in developing NK cells.^{23,24}

Herein, we examined the role of SFRs in the generation of adaptive NK cells, using the MCMV model. In adoptive transfer experiments using Ly49H⁺ NK cells lacking one or more SFRs, we observed that Ly49H⁺ NK cells devoid of CD48 showed a marked defect in expansion after MCMV infection compared with wild-type Ly49H⁺ NK cells. The impact of CD48 deficiency in NK cells was mimicked when host macrophages lacked the counter-receptor of CD48, that is, 2B4. The 2B4-CD48 axis acted by suppressing phagocytosis of NK cells by activated macrophages through inhibition of the pro-phagocytic integrin LFA-1 expressed on macrophages. These data demonstrate a key role of macrophages, as well as of the 2B4-CD48 axis, in controlling the expansion of adaptive NK cells after MCMV infection.

RESULTS

SFRs are required for expansion of Ly49H⁺ NK cells after MCMV infection

To test the involvement of SFRs in the generation of adaptive NK cells, we used the MCMV model.^{11,25} Thus, “recipient” mice lack-

ing Ly49H (Ly49H knockout [KO] mice) were adoptively administered equal numbers of “donor” NK cells from mice expressing or not expressing canonical SFRs plus CD48 (the “SFR KO” mouse) (Figure 1A). The SFR KO mouse was previously generated by deletion of the entire *Slam* locus on mouse chromosome 1 in the C57BL/6 (B6) background.²⁶ It displayed no alteration in NK cell numbers, development, or maturation.²⁶ As was the case for wild-type mice, ~60% of splenic NK cells from SFR KO mice were Ly49H⁺ (Figure 1B).

One day after adoptive transfer of NK cells, mice were infected with MCMV and, at various times after infection, the proportions and numbers of wild-type and SFR KO Ly49H⁺ NK cells in blood and spleen were determined. Of note, long-lived adaptive NK cells are considered to be formed by day 35 post-infection.^{17,27,28} As expected, wild-type Ly49H⁺ NK cells (identified as NK1.1⁺, TCRβ⁻, Ly49H⁺, CD48⁺) showed robust expansion in blood at day 7 after MCMV infection (Figures 1C and S1A). In comparison, SFR KO Ly49H⁺ NK cells (NK1.1⁺, TCRβ⁻, Ly49H⁺, CD48⁻), which were identified by a lack of CD48 normally expressed on all NK cells,²⁶ displayed severely impaired accumulation, both in proportions and in numbers (reduced by ~90%–95%). This difference persisted over the long term (up to day 35 or 56) and was also noted in spleen (Figures 1C and 1D).

Hence, loss of all canonical SFRs, in addition to CD48, resulted in a rapid and pronounced defect in expansion of adaptive Ly49H⁺ NK cells in response to MCMV infection.

CD48 is predominantly involved in MCMV-induced expansion of Ly49H⁺ NK cells

To identify the SFR(s) responsible for this defect, mice specifically lacking the SFRs expressed in NK cells, that is, 2B4 (2B4 KO), its ligand CD48 (CD48 KO), SLAMF7 (SLAMF7 KO), SLAMF1 (SLAMF1 KO), or SLAMF6 (SLAMF6 KO), were tested (Figures 2A–2E). Unless indicated, SJL.B6 NK cells, which expressed CD45.1, were used as wild-type NK cells in these experiments to enable their distinction from the mutant NK cells, which expressed CD45.2.

Unlike SFR KO Ly49H⁺ NK cells, 2B4 KO Ly49H⁺ NK cells (identified as NK1.1⁺, TCRβ⁻, Ly49H⁺, CD45.1⁻) displayed increased (by ~10%–20%), rather than diminished, expansion following MCMV infection compared with wild-type Ly49H⁺ NK cells (NK1.1⁺, TCRβ⁻, Ly49H⁺, CD45.1⁺) (Figure 2A). SLAMF1 KO and SLAMF6 KO Ly49H⁺ NK cells displayed minimal differences compared with WT Ly49H⁺ NK cells (Figures 2D and 2E). In contrast, like SFR KO Ly49H⁺ NK cells, CD48 KO Ly49H⁺ NK cells (NK1.1⁺, TCRβ⁻, Ly49H⁺, CD48⁻) exhibited a marked reduction (by ~80%–90%) in expansion compared with wild-type Ly49H⁺ NK cells (NK1.1⁺, TCRβ⁻, Ly49H⁺, CD48⁺) (Figures 2B and S1D). This deficit was maximal at day 7, persisted over the long term, and was seen in blood, spleen, liver, lung, lymph node, and bone marrow (Figure S1B and S1C). Importantly, no defect in proportions or numbers of CD48 KO Ly49H⁺ NK cells was noted in the absence of MCMV infection, implying that the expansion defect was revealed by MCMV infection (Figure S1E). Also, like SFR KO mice, CD48 KO mice showed no abnormalities in NK cell development or maturation, as indicated by

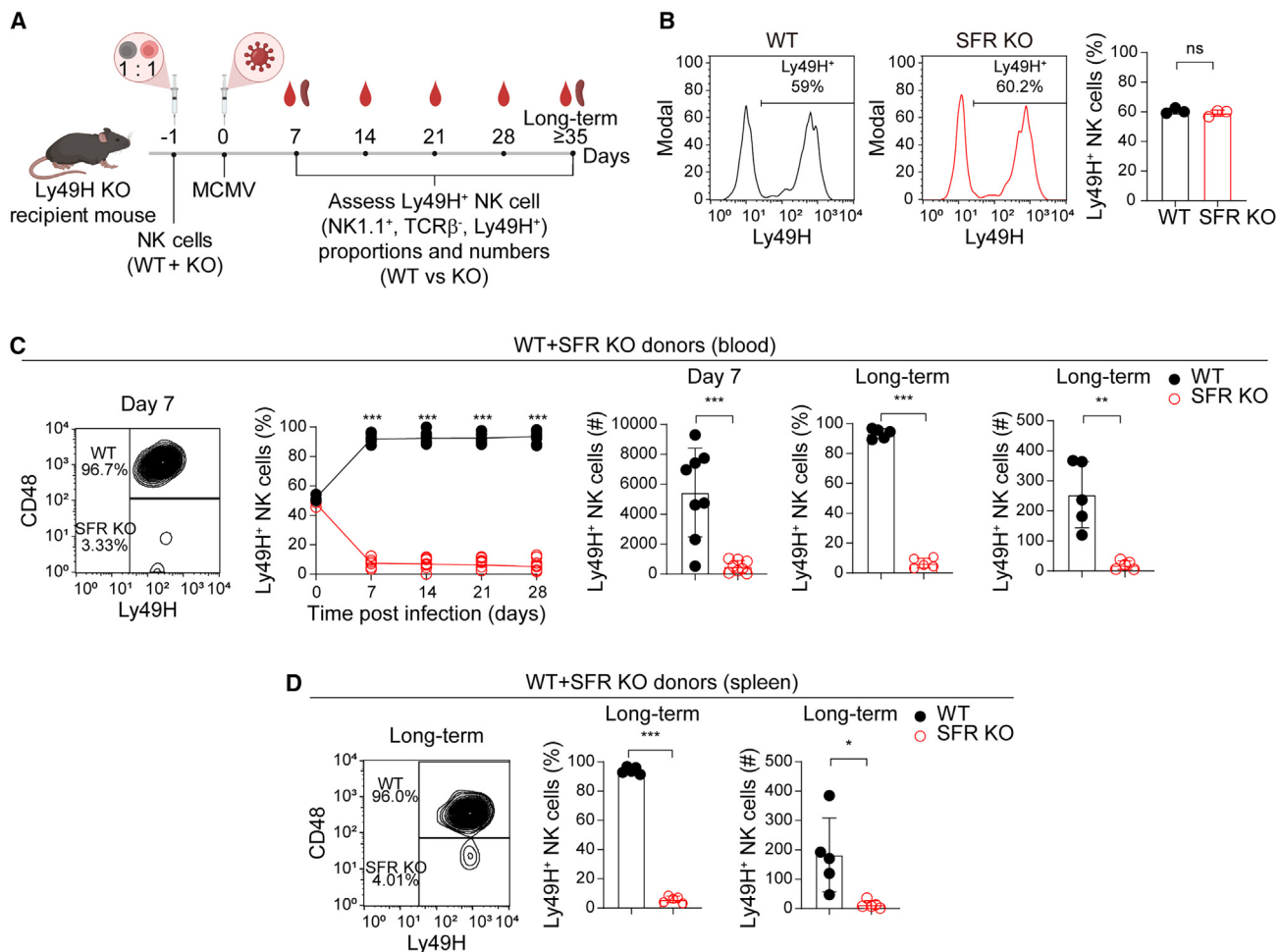


Figure 1. Involvement of SFRs in the expansion of Ly49H⁺ NK cells following MCMV infection

(A) Schematic diagram of adoptive transfer experiment. On day -1 (1 day before infection), equal numbers of Ly49H⁺ NK cells from wild-type (WT) mice and mice lacking all SLAM family receptors (SFRs) plus CD48 (SFR knockout [KO] mice) were mixed and injected intravenously into Ly49H KO recipient mice. On day 0, 7.5 × 10² pfu of MCMV was injected intraperitoneally into recipients. The proportions and numbers of WT and SFR KO Ly49H⁺ NK cells were analyzed in blood or spleen at the indicated time points. Long-term results were assessed at either day 35 or day 56.

(B) From left to right: first two graphs, representative flow cytometry analyses of Ly49H expression on freshly isolated WT or SFR KO splenic NK cells in donor mice on day -1; third graph, statistical analysis of multiple independent mice (n = 3).

(C) From left to right: first graph, representative flow cytometry analysis of the proportions of WT (CD48⁺) and SFR KO (CD48⁻) Ly49H⁺ NK cells in the blood of recipient mice at day 7. Second graph, statistics of the proportions at various time points (n = 8). Third graph, numbers of WT and SFR KO Ly49H⁺ NK cells per million lymphocytes at day 7 (n = 8). Fourth graph, the proportions at day 35 (n = 5). Fifth graph, numbers of WT and SFR KO Ly49H⁺ NK cells per million lymphocytes in blood at day 35 (n = 5).

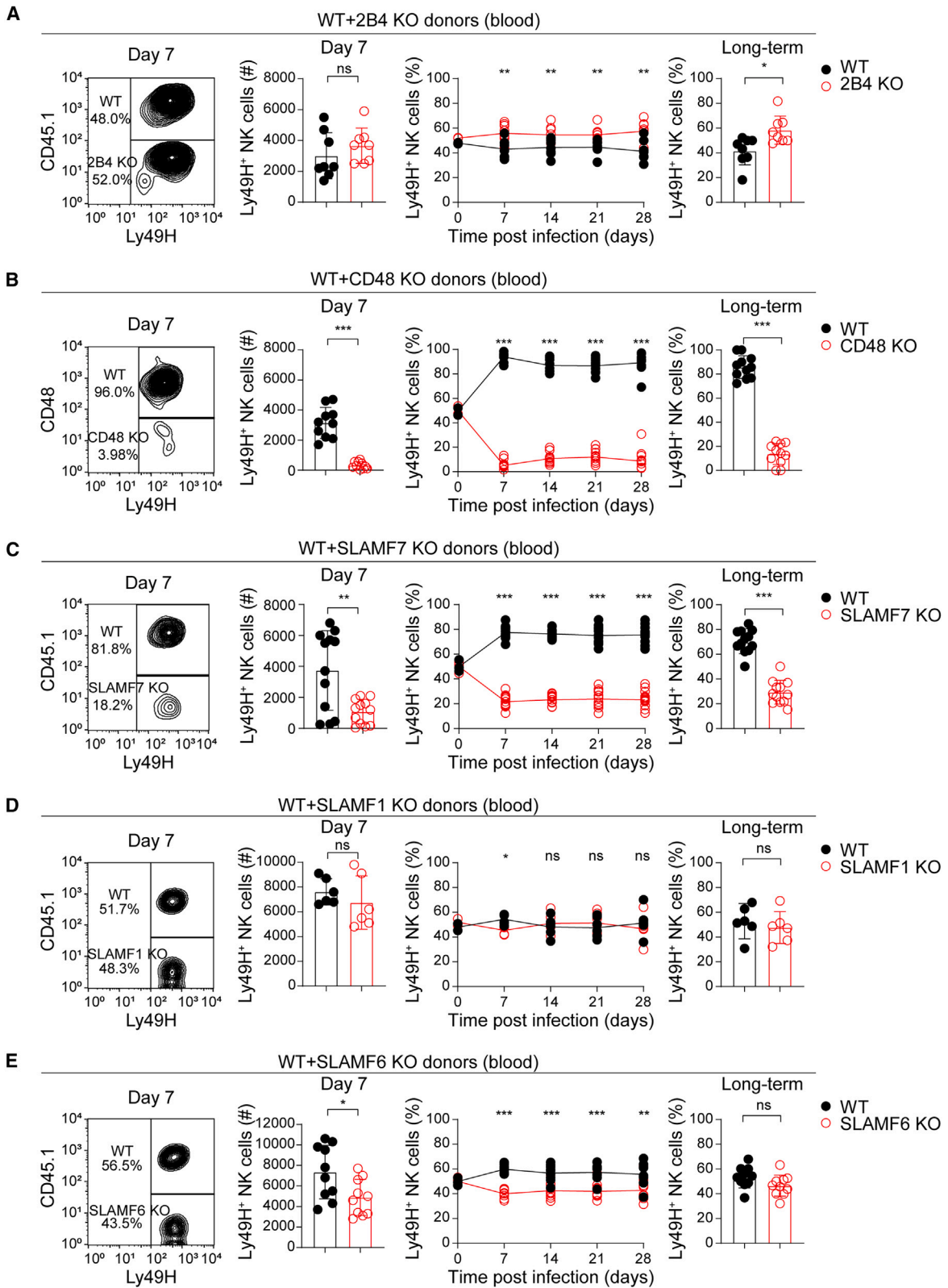
(D) Same as (C), except that NK cell proportions and numbers were assessed in the spleen after mice were euthanized at day 35 (n = 5). Statistical analyses were conducted using unpaired t tests (two-tailed), except in graphs displaying data with multiple time points, for which multiple t tests were employed. Each symbol represents an individual mouse; error bars depict the mean with SD. *p ≤ 0.05, **p ≤ 0.01, ***p ≤ 0.001; ns, not significant. Data are representative of three (B), three (C, first to third graphs), two (C, fourth and fifth graphs), and two (D) independent experiments; two or three recipient mice were injected with purified NK cells in each independent experiment. See also Figure S1.

analyses of various NK cell markers, including maturation markers CD27 and CD11b (Figures S2A and S2B).

Albeit to a much lesser extent than CD48 KO Ly49H⁺ NK cells, SLAMF7 KO Ly49H⁺ NK cells also displayed a defect in expansion (numbers reduced by ~40%) compared with wild-type Ly49H⁺ NK cells (Figures 2C and S3A). The much less pronounced defect of SLAMF7 KO Ly49H⁺ NK cells, compared with CD48 KO Ly49H⁺ NK cells, was confirmed when both cell

types were co-injected in the same adoptive transfer experiment (Figure S2C).

As 2B4 KO Ly49H⁺ NK cells did not show the same expansion defect as CD48 KO Ly49H⁺ NK cells, we ascertained if CD48 was mediating its effect by triggering CD2, an alternative counter-receptor for CD48 also expressed on NK cells.²⁹ Although a small decrease (by ~20%) in expansion of CD2 KO Ly49H⁺ NK cells (identified as NK1.1⁺, TCRβ⁻, Ly49H⁺, CD2⁻) was seen upon



(legend on next page)

MCMV infection, compared with wild-type Ly49H⁺ NK cells (NK1.1⁺, TCRβ⁻, Ly49H⁺, CD2⁺), this defect was much milder than that of CD48 KO Ly49H⁺ NK cells (Figure S3B).

Last, we analyzed the impact of MCMV infection on the expression levels of CD48, as well as other SFRs, on NK cells using flow cytometry. Cell-surface expression of CD48 was augmented on Ly49H⁺ NK cells at day 4 and day 7 post-infection compared with non-infected mice (Figures S3C–S3F). Expression of SLAMF7 and 2B4 was also augmented at both time points, whereas an increase in expression of SLAMF6 and Ly-9 was noted at day 4, but not at day 7.

Thus, CD48 largely mediated the role of SFRs in the expansion of adaptive Ly49H⁺ NK cells during MCMV infection. This function was not observed in the absence of MCMV infection and did not require expression of the CD48 counter-receptors 2B4 and CD2 on Ly49H⁺ NK cells. A smaller role was played by SLAMF7.

CD48 has little or no impact on NK cell activation and proliferation after MCMV infection

To examine if the lack of CD48 compromised the initial activation or proliferation of Ly49H⁺ NK cells, activation markers CD69 and KLRG1, as well as proliferation marker Ki67,^{25,30,31} were measured. At day 4 and day 7 post-infection, there was little or no difference in upregulated expression of CD69, KLRG1, and Ki67 between wild-type and CD48 KO Ly49H⁺ NK cells (Figures 3A–3C, S4A, and S4B). A small decrease in the expression of KLRG1 and Ki67 was noted, but it likely reflected the changes in NK cell subsets seen in response to infection, as will be described below (Figures 3D and S4C).

In addition to activation and proliferation of Ly49H⁺ NK cells, MCMV infection results in differentiation of Ly49H⁺ NK cells toward more mature subsets, that is, CD27⁺CD11b⁺ (stage [S] 3) and CD27⁻CD11b⁺ (S4) NK cells.³² Using flow cytometry, we observed that the numbers of S3 and S4 CD48 KO Ly49H⁺ NK cells after MCMV infection were markedly reduced compared with wild-type Ly49H⁺ cells (Figures 3D and S4C). In contrast, no reduction in the numbers of S1 and S2 Ly49H⁺ NK cells was seen. As a consequence of these changes, the proportions of S1 and S2 cells in CD48 KO Ly49H⁺ NK cells were augmented. The reduction in S3 and S4 NK cells was seen as early as day 4,

even before the massive expansion of NK cells, and was accentuated at day 7, when NK cell expansion had largely taken place. As S3 and S4 NK cells express higher levels of activation markers,¹³ the predominant loss of these two subsets likely explained the slightly reduced expression of KLRG1 and Ki67 on CD48 KO Ly49H⁺ NK cells compared with wild-type Ly49H⁺ NK cells (Figures 3B and 3C).

Most Ly49H⁺ NK cells activated during MCMV infection are eliminated through a poorly understood suppression phase involving cell death.¹¹ At day 4 and day 7 post-infection, there was little or no increase in the proportions of CD48 KO Ly49H⁺ cells displaying activated caspases, which are reflective of apoptosis,³³ compared with wild-type Ly49H⁺ NK cells (Figures 3E and S4D).

Thus, CD48 deficiency on NK cells resulted in a disproportionate loss of mature NK cell subsets, S3 and S4. However, it had little or no impact on NK cell activation, proliferation, or death in response to MCMV infection, suggesting an NK cell-extrinsic mechanism.

2B4 on recipient cells is required for expansion of Ly49H⁺ NK cells after MCMV infection

Although the presence of 2B4 and CD2 on transferred NK cells played little or no role in the expansion of Ly49H⁺ NK cells, it was possible that 2B4, CD2, or both on recipient cells were involved. To address this idea, adoptive transfer experiments were performed using wild-type and CD48 KO NK cells as above, but using 2B4 KO mice or CD2 KO mice as recipients (Figure 4A). All recipient mice were also engineered to be deficient in Ly49H.

When 2B4-Ly49H double-knockout (DKO) mice were used as recipients, the proportions of wild-type and CD48 KO Ly49H⁺ NK cells in response to MCMV infection were nearly equivalent (Figure 4B). At some of the time points, CD48 KO Ly49H⁺ NK cells were actually slightly more abundant than wild-type Ly49H⁺ NK cells (Figure 4C). However, when NK cell numbers were assessed, both wild-type and CD48 KO Ly49H⁺ NK cells displayed dramatically reduced abundance (by ~90%) (Figure 4D). When CD2-Ly49H DKO mice were used as recipients, the difference in expansion of wild-type and CD48 KO Ly49H⁺ NK cells was similar to that noted in Ly49H KO hosts (Figure 4E).

Figure 2. Contribution of CD48 to the expansion of Ly49H⁺ NK cells following MCMV infection

(A) On day -1 (1 day before infection), equal numbers of Ly49H⁺ NK cells from WT (B6.SJL) and 2B4 KO donors were mixed and injected into Ly49H KO mice. On day 0, 7.5×10^2 pfu of MCMV was injected intraperitoneally into recipients. The proportions of WT versus 2B4 KO NK cells in the Ly49H⁺ population in the blood of recipient mice were analyzed at the indicated time points. From left to right: first graph, representative flow cytometry analysis of the proportions of WT (CD45.1⁺) and 2B4 KO (CD45.1⁻) Ly49H⁺ NK cells at day 7. Second graph, numbers of WT and 2B4 KO Ly49H⁺ NK cells per million blood lymphocytes at day 7 (n = 8). Third graph, proportions of the cells at various indicated time points (n = 8). Fourth graph, proportions of the cells at day 35 (n = 8).

(B) Same as (A), except that equal numbers of Ly49H⁺ NK cells from WT (B6) and CD48 KO donors were mixed and injected into Ly49H KO mice and CD48 was used as a marker to distinguish WT (CD48⁺) and CD48 KO (CD48⁻) cells. Long-term results were assessed at day 56 (second graph, n = 10; third and fourth graphs, n = 11).

(C) Same as (A), except that equal numbers of Ly49H⁺ NK cells from WT (B6.SJL) and SLAMF7 KO donors were mixed and injected into Ly49H KO mice. Long-term results were assessed at day 56 (second graph, n = 12; third graph, n = 13; fourth graph, n = 12).

(D) Same as (A), except that equal numbers of Ly49H⁺ NK cells from WT (B6.SJL) and SLAMF1 KO donors were mixed and injected into Ly49H KO mice. Long-term results were assessed at day 35 (n = 6).

(E) Same as (A), except that equal numbers of Ly49H⁺ NK cells from WT (B6.SJL) and SLAMF6 KO donors were mixed and injected into Ly49H KO mice. Long-term results were assessed at day 35 (n = 10). Statistical analyses were conducted using unpaired t tests (two-tailed), except in graphs displaying data with multiple time points, for which multiple t tests were employed. Each symbol represents an individual mouse; error bars depict the mean with SD. *p ≤ 0.05, **p ≤ 0.01, ***p ≤ 0.001; ns, not significant. Data are representative of two (A), three (B), four (C), two (D), and three (E) independent experiments; two to four recipient mice were injected with purified NK cells in each independent experiment. See also Figures S1–S3.

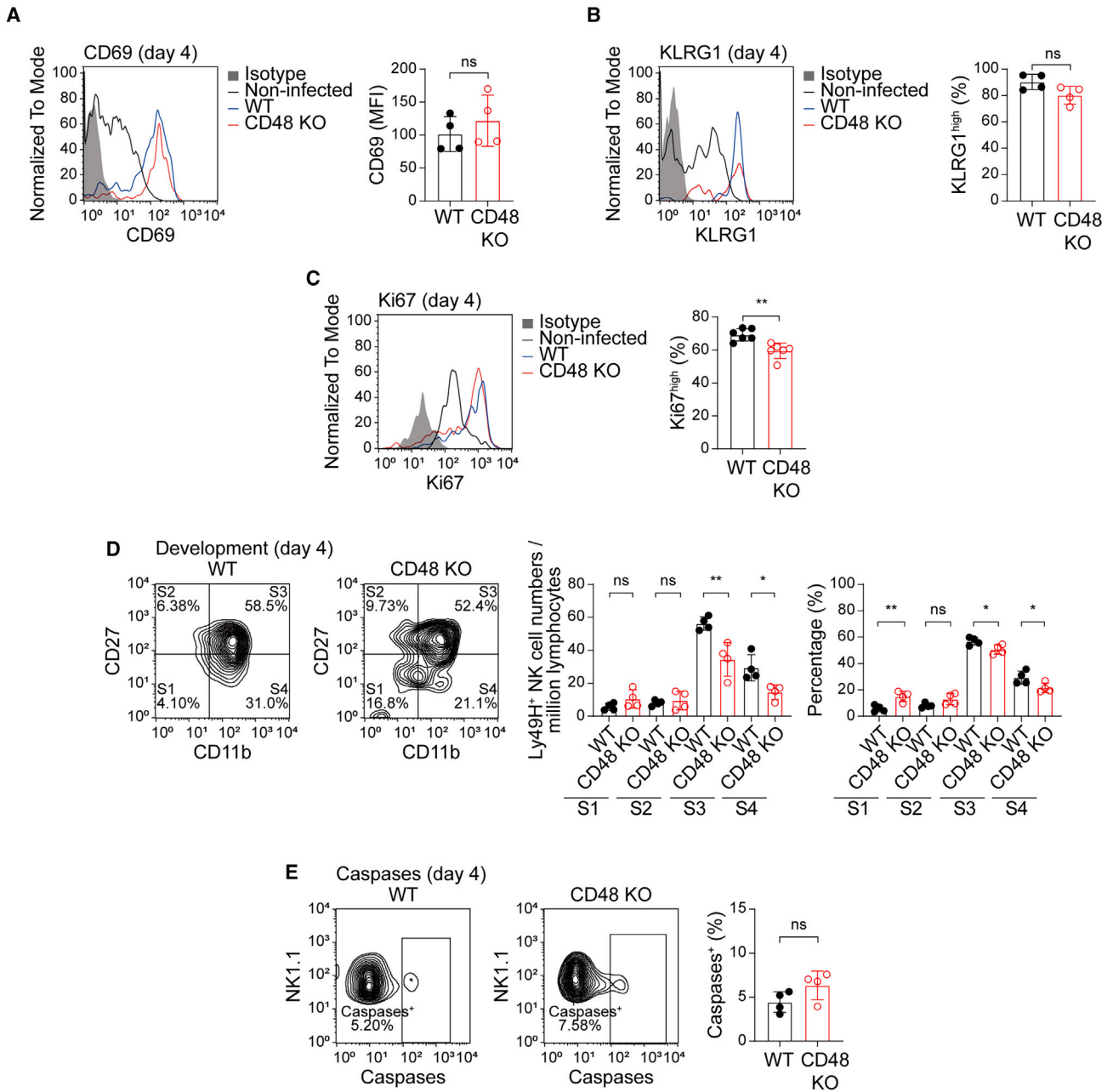


Figure 3. Minimal effect of CD48 deficiency on NK cell activation and proliferation

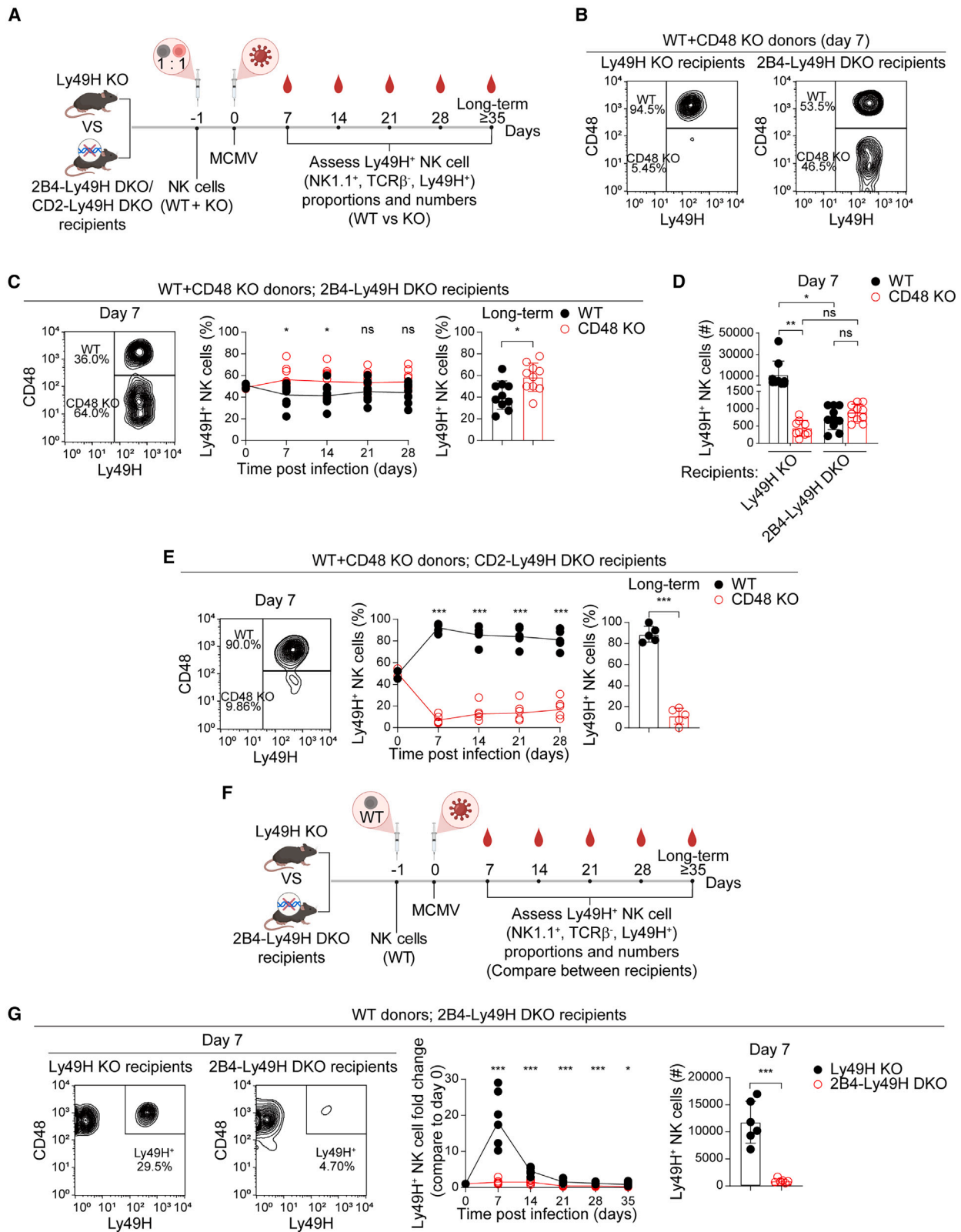
(A) Equal numbers of Ly49H⁺ NK cells from WT and CD48 KO donors were mixed and injected into Ly49H KO mice following MCMV infection. Expression of various markers was determined on freshly isolated WT or CD48 KO splenic Ly49H⁺ NK cells on day 4. Left, representative flow cytometry analysis of activating marker CD69 expression on non-infected controls (black), WT (blue), and CD48 KO (red) Ly49H⁺ NK cells; isotype controls are shown in gray. Right, statistical analysis of mean fluorescence intensity (MFI) of CD69 (n = 4).

(B) Same as (A), except that KLRG1 expression was assessed (n = 4).

(C) Same as (A), except that Ki67 expression was assessed by intracellular staining (n = 6).

(D) Same as (A), except that the expression of CD11b and CD27 was assessed to check the development of Ly49H⁺ NK cells. Stage 1 (S1), CD11b⁻/CD27⁻; stage 2 (S2), CD11b⁻/CD27⁺; stage 3 (S3), CD11b⁺/CD27⁺; stage 4 (S4), CD11b⁺/CD27⁻ (n = 4).

(E) Same as (A), except that activated caspases were assessed by intracellular staining (n = 4). Statistical analyses were conducted using unpaired t tests (two-tailed). Each symbol represents an individual mouse; error bars depict the mean with SD. *p ≤ 0.05, **p ≤ 0.01, ***p ≤ 0.001; ns, not significant. Data are representative of two (A), two (B), three (C), two (D), and two (E) independent experiments; one to three recipient mice were injected with purified NK cells in each independent experiment. See also Figure S4.



(legend on next page)

To quantify more precisely the impact of 2B4 deficiency in recipient mice, wild-type Ly49H⁺ NK cells alone were transferred into 2B4-Ly49H DKO or Ly49H KO hosts (Figure 4F). When injected into 2B4-Ly49H DKO hosts, wild-type Ly49H⁺ NK cells displayed a marked decrease (by >95%) in expansion following MCMV infection compared with Ly49H KO hosts (Figure 4G). This defect was seen as early as day 7 post-infection.

Therefore, loss of 2B4, but not of CD2, in the host mimicked the impact of loss of CD48 on adaptive Ly49H⁺ NK cells during MCMV infection.

Evidence that macrophages restrict expansion of Ly49H⁺ NK cells during MCMV infection

2B4 is expressed on NK cells, macrophages, dendritic cells, and some CD8⁺ T cells. Previous studies documented an inhibitory role of 2B4 in NK cells, at least in mice, as well as in macrophages.^{26,34} When 2B4 on mouse NK cells is engaged by CD48 on target cells, including on adjacent NK cells, it suppresses cytotoxicity.³⁵ Killing of NK cells by other NK cells, so-called “fratricide,” underlies the reduced expansion of Ly49H⁺ NK cells in the absence of type I IFN signaling in Ly49H⁺ NK cells.¹⁷

To ascertain if CD48 on transferred Ly49H⁺ NK cells was acting by engaging 2B4 on host NK cells, we could not use classical NK cell depletion reagents such as anti-asialo-GM1 or anti-NK1.1 antibodies, as these antibodies would also deplete the transferred NK cells. Thus, we used as the recipient mouse the RAG-2-IL-2 receptor common γ chain (RAG-2-IL-2R γ) DKO mouse, which lacks NK cells^{36,37} (Figure 5A). As the RAG-2-IL-2R γ DKO mouse also lacks mature T cells and B cells, we used as control the RAG-1 KO mouse, which is devoid only of mature T cells and B cells. The RAG-1 KO mouse was bred with the Ly49H KO mouse, to eliminate Ly49H⁺ on host NK cells.

When injected with wild-type and CD48 KO Ly49H⁺ NK cells, RAG-2-IL-2R γ DKO hosts still showed a severe defect in the expansion of CD48 KO Ly49H⁺ NK cells following MCMV infection compared with wild-type Ly49H⁺ NK cells (Figures 5B and S5A). A similar deficit was noted in RAG-1-Ly49H DKO mice (Figures 5C and S5B). Hence, host NK cells were not involved in the compromised expansion of CD48 KO Ly49H⁺ NK cells. Although CD48 KO Ly49H⁺ NK cells were much more diminished

than wild-type Ly49H⁺ NK cells in proportions and numbers in the RAG-1-deficient host mice, wild-type Ly49H⁺ NK cells were also reduced in numbers compared with Ly49H KO host mice (Figure S5C). This phenomenon was previously ascribed to a requirement of host CD8⁺ T cells for avoiding Ly49H⁺ NK cell exhaustion during MCMV infection.³⁸

The notion that 2B4 is inhibitory in macrophages was suggested by the finding that engagement of 2B4 on macrophages by CD48 on T cells prevented phagocytosis of T cells.³⁴ To ascertain if macrophages were involved in the reduced expansion of CD48 KO Ly49H⁺ NK cells, host macrophages were depleted using two complementary approaches. First, recipient mice were treated for 3 weeks with blocking anti-colony-stimulating factor-1 receptor (CSF-1R) antibodies, which prevent differentiation of monocytes into macrophages.³⁹ Anti-CSF-1R antibodies resulted in a partial reduction (by ~75%) of splenic macrophage (identified as B220⁻, TCR β ⁻, NK1.1⁻, F4/80⁺, CD11b^{-/lo}) compared with control antibodies (Figures 5D and S5D). They also partially corrected the expansion defect of CD48 KO Ly49H⁺ NK cells in spleen and blood compared with wild-type Ly49H⁺ NK cells (Figures 5E and S5E).

Second, recipient mice were treated with clodronate encapsulated in liposomes, which eliminates macrophages by direct cytotoxicity.⁴⁰ Compared with control liposomes, clodronate-containing liposomes yielded a >90% depletion of splenic macrophages (Figure 5F). They also ameliorated the defect in expansion of CD48 KO Ly49H⁺ NK cells compared with wild-type Ly49H⁺ NK cells (Figure 5G). The greater efficacy of clodronate at restoring expansion of CD48 KO Ly49H⁺ NK cells, compared with blocking anti-CSF-1R antibodies, is likely related to its greater capacity to deplete macrophages (Figures 5D–5G).

Hence, these data supported the idea that host macrophages, but not host NK cells, were responsible at least in part for the reduced expansion of CD48 KO Ly49H⁺ NK cells during MCMV infection.

2B4-CD48 prevents phagocytosis of activated NK cells during MCMV infection

To test if the 2B4-CD48 axis was preventing phagocytosis of NK cells by macrophages in the context of MCMV infection, an

Figure 4. Recipient cell-expressed 2B4 is necessary for the expansion of Ly49H⁺ NK cells following MCMV infection

(A) Schematic diagram of adoptive transfer experiment. On day -1 (1 day before infection), equal numbers of Ly49H⁺ NK cells from WT and CD48 KO mice were mixed and injected intravenously into Ly49H KO, 2B4-Ly49H DKO, or CD2-Ly49H DKO recipient mice. On day 0, 7.5 × 10² pfu of MCMV was injected intraperitoneally into recipients. The proportions and numbers of WT and CD48 KO Ly49H⁺ NK cell populations were analyzed in blood at the indicated time points. (B) Representative flow cytometry analysis of the proportions of WT (CD48⁺) and CD48 KO (CD48⁻) Ly49H⁺ NK cells in Ly49H KO mice and 2B4-Ly49H DKO mice is depicted.

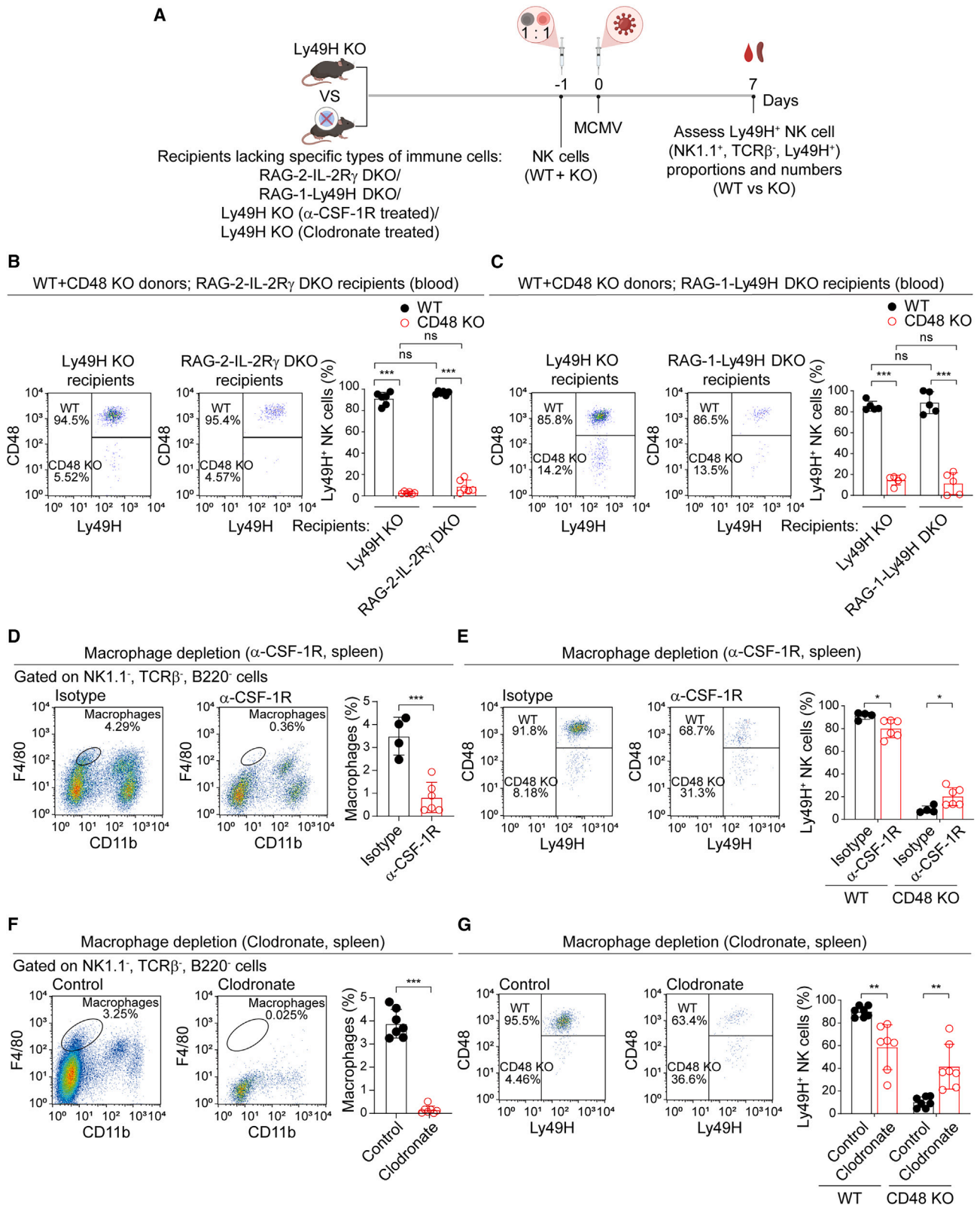
(C) From left to right: first graph, representative flow cytometry analysis of the proportions of WT and CD48 KO Ly49H⁺ NK cells in 2B4-Ly49H DKO recipient mice at day 7. Second graph, the proportions at various time points are depicted (n = 10). Third graph, long-term results at day 35 (n = 10).

(D) Same as (B), except that the numbers of WT and CD48 KO Ly49H⁺ NK cells per million lymphocytes are depicted (n = 10).

(E) Same as (C), except that the proportions in CD2-Ly49H DKO recipient mice are depicted. Long-term results were assessed at day 35 (n = 5).

(F) Same as (A), except that only WT Ly49H⁺ NK cells were injected into Ly49H KO or 2B4-Ly49H DKO recipient mice.

(G) From left to right: first and second graphs, proportions of Ly49H⁺ NK cells in the total NK cell population (NK1.1⁺, TCR β ⁻) in the blood of Ly49H KO and 2B4-Ly49H DKO recipient mice are depicted. Third graph, fold change in Ly49H⁺ proportions in the total NK cell population of Ly49H KO and 2B4-Ly49H DKO recipient mice at indicated time points compared with day 0 (n = 6). Fourth graph, numbers of Ly49H⁺ NK cells per million lymphocytes at day 7 (n = 6). Statistical analyses were conducted using unpaired t tests (two-tailed), except in graphs displaying data with multiple time points, for which multiple t tests were employed. In addition, in graphs involving comparisons of more than two groups, one-way ANOVA followed by Tukey’s multiple comparisons test were used. Each symbol represents an individual mouse; error bars depict the mean with SD. *p ≤ 0.05, **p ≤ 0.01, ***p ≤ 0.001; ns, not significant. Data are representative of four (B), four (C), four (D), two (E), and two (G) independent experiments; two or three recipient mice were injected with purified NK cells in each independent experiment.



(legend on next page)

in vitro model of MCMV infection was developed according to a published protocol.⁴¹ Mouse bone marrow-derived macrophages (BMDMs) were infected *in vitro* with an MCMV variant encoding green fluorescent protein (GFP) (Figure 6A). Monitoring of GFP expression enabled the distinction of “infected” macrophages (GFP⁺) from “bystanding” macrophages (GFP⁻), which are not infected but are activated by soluble factors produced during MCMV infection (Figure 6B). BMDMs not subjected to MCMV infection (“non-infected”) were used as controls (Figure 6A). As reported, following MCMV infection, infected GFP⁺ BMDMs exhibited loss of surface expression of F4/80 and CD45 compared with bystanding BMDMs, reflecting macrophage dedifferentiation (Figure 6C).

Twenty-four hours after infection, microscopy-based phagocytosis assays were performed, using as targets wild-type or CD48 KO NK cells previously activated with IL-12, IL-15, and IL-18 and labeled with CellTrace violet (CTV) (Figure 6A). NK cells were activated using cytokines, rather than antibodies against activating receptors present on NK cells, to avoid phagocytosis of NK cells upon triggering of Fc receptors on macrophages. With non-infected macrophages, the efficiency of phagocytosis was quite low (~5%–7%). It was slightly greater toward CD48 KO NK cells compared with wild-type NK cells (Figure 6D). After MCMV infection, though, BMDMs had a much higher efficiency of phagocytosis, especially toward CD48 KO NK cells (~25%), compared with wild-type NK cells (~15%). This effect was solely seen in bystanding BMDMs. GFP⁺ BMDMs, which were infected by MCMV, exhibited little phagocytosis, in keeping with the previous report that these cells were incapable of phagocytosing latex particles.⁴¹

Next, we tested phagocytosis of wild-type NK cells incubated in the presence of wild-type or 2B4 KO BMDMs. Compared with wild-type bystanding BMDMs, the 2B4 KO bystanding BMDMs displayed greater phagocytosis of wild-type NK cells (~25% versus ~15%) (Figure 6E). A small increase in phagocytosis was also seen in non-infected 2B4 KO BMDMs compared with wild-type BMDMs (~10% versus ~7%).

Therefore, loss of CD48 on NK cells or loss of 2B4 on macrophages resulted in greater phagocytosis of activated NK cells by

macrophages during MCMV infection. Bystanding macrophages, but not infected macrophages, were responsible for this increase.

Phagocytosis of NK cells regulated by 2B4-CD48 is mediated by integrin LFA-1

Phagocytosis requires not only relief of the inhibitory function of receptors like 2B4, but also triggering of pro-phagocytic “eat me” receptors.^{34,42} Pro-phagocytic receptors include receptors for the Fc portion of antibodies (FcRs), integrin Mac-1 (CD11b), and SLAMF7, which recognize antibodies, complement, and SLAMF7, respectively, on target cells. During inflammation, integrins LFA-1 (CD11a) and CD11c can also act as pro-phagocytic receptors, triggered by as-yet unknown ligands on target cells.⁴² Mac-1, LFA-1, and CD11c associate with the same signaling subunit, known as CD18 or β 2 integrin.⁴³

To identify the pro-phagocytic receptor(s) on macrophages involved in elimination of CD48 KO NK cells, we first examined the expression of known pro-phagocytic receptors in the presence or in the absence of MCMV infection *in vitro*. Given that exogenous antibodies were not used in our phagocytosis assays, it was unlikely that FcRs were involved. Moreover, as SFR KO NK cells, which lacked not only CD48 but also SLAMF7, displayed augmented elimination *in vivo*, it was improbable that SLAMF7 was implicated. Consequently, we focused on integrins.

Compared with non-infected BMDMs, bystanding BMDMs displayed an increase (~3- to 4-fold) in expression of CD11a, as well as of LFA-1 (which represents the CD11a-CD18 heterodimer) (Figures 7A and 7B). A small increase (~2-fold) in expression of CD18 was also seen. In contrast, there was reduced expression of CD11b (by ~80%), and only low levels of CD11c were seen. Of note, bystanding and infected BMDMs also showed a diminution in expression of 2B4 (by ~70%–80%) and CD48 (by ~10%–30%) compared with non-infected BMDMs.

In the light of these findings, we first studied the impact of antibody-mediated blockade of CD11a or CD18 on phagocytosis. Compared with control antibodies, blocking anti-CD11a antibodies or blocking anti-CD18 antibodies markedly reduced the ability of bystanding macrophages to phagocytose wild-type and CD48 KO NK cells (Figures 7C and 7D). The augmented

Figure 5. Macrophages limit the expansion of Ly49H⁺ NK cells

(A) Schematic diagram of adoptive transfer experiment. On day -1 (1 day before infection), equal numbers of Ly49H⁺ NK cells from WT mice and CD48 KO mice were mixed and injected intravenously into Ly49H KO recipients versus recipients lacking specific types of immune cells, including RAG-2-IL-2R γ DKO mice, RAG-1-Ly49H DKO mice, or Ly49H KO mice treated with α -CSF-1R or clodronate-containing liposomes. On day 0, 7.5×10^2 pfu of MCMV was injected intraperitoneally into recipients. The proportions and numbers of WT and CD48 KO NK cells in the Ly49H⁺ NK cell population were analyzed in the blood or spleen at day 7.

(B) The proportions of WT versus CD48 KO Ly49H⁺ NK cells in the blood of Ly49H KO or RAG-2-IL-2R γ DKO recipient mice were analyzed at day 7. From left to right: first two graphs, representative flow cytometry analyses are depicted. Third graph, statistical analysis for multiple independent mice (n = 6).

(C) Same as (B), except that the Ly49H KO or RAG-1-Ly49H DKO recipient mice were used (n = 5).

(D) Macrophage depletion in Ly49H KO recipient mice by injection of anti-CSF-1R antibody before and during the adoptive transfer experiments. Control group was treated with isotype antibody. From left to right: first two graphs, representative flow cytometry analyses of the macrophage depletion efficiency in splenocytes at day 7 are depicted; macrophages were identified as B220⁻, TCR β ⁻, NK1.1⁻, F4/80⁺, CD11b^{-/lo} cells, and the percentage represents the proportion of macrophages in the B220⁻, TCR β ⁻, NK1.1⁻ population. Third graph, statistical analysis for multiple independent mice (n = 4 for isotype control; n = 6 for α -CSF-1R).

(E) Same as (D), except that the proportions of WT and CD48 KO Ly49H⁺ NK cells were analyzed (n = 4 for isotype control; n = 6 for α -CSF-1R).

(F) Same as (D), except that macrophages were depleted by injection of clodronate encapsulated in liposomes before and during the adoptive transfer experiments. Control group was treated with control liposomes (n = 7).

(G) Same as (F), except the proportions of WT and CD48 KO Ly49H⁺ NK cells were analyzed (n = 7). Statistical analyses were conducted using unpaired t tests (two-tailed), except in graphs that involved comparisons of more than two groups, for which one-way ANOVA followed by Tukey’s multiple comparisons test were employed. Each symbol represents an individual mouse; error bars depict the mean with SD. *p \leq 0.05, **p \leq 0.01, ***p \leq 0.001; ns, not significant. Data are representative of two independent experiments; two to four recipient mice were injected with purified NK cells in each independent experiment. See also Figure S5.

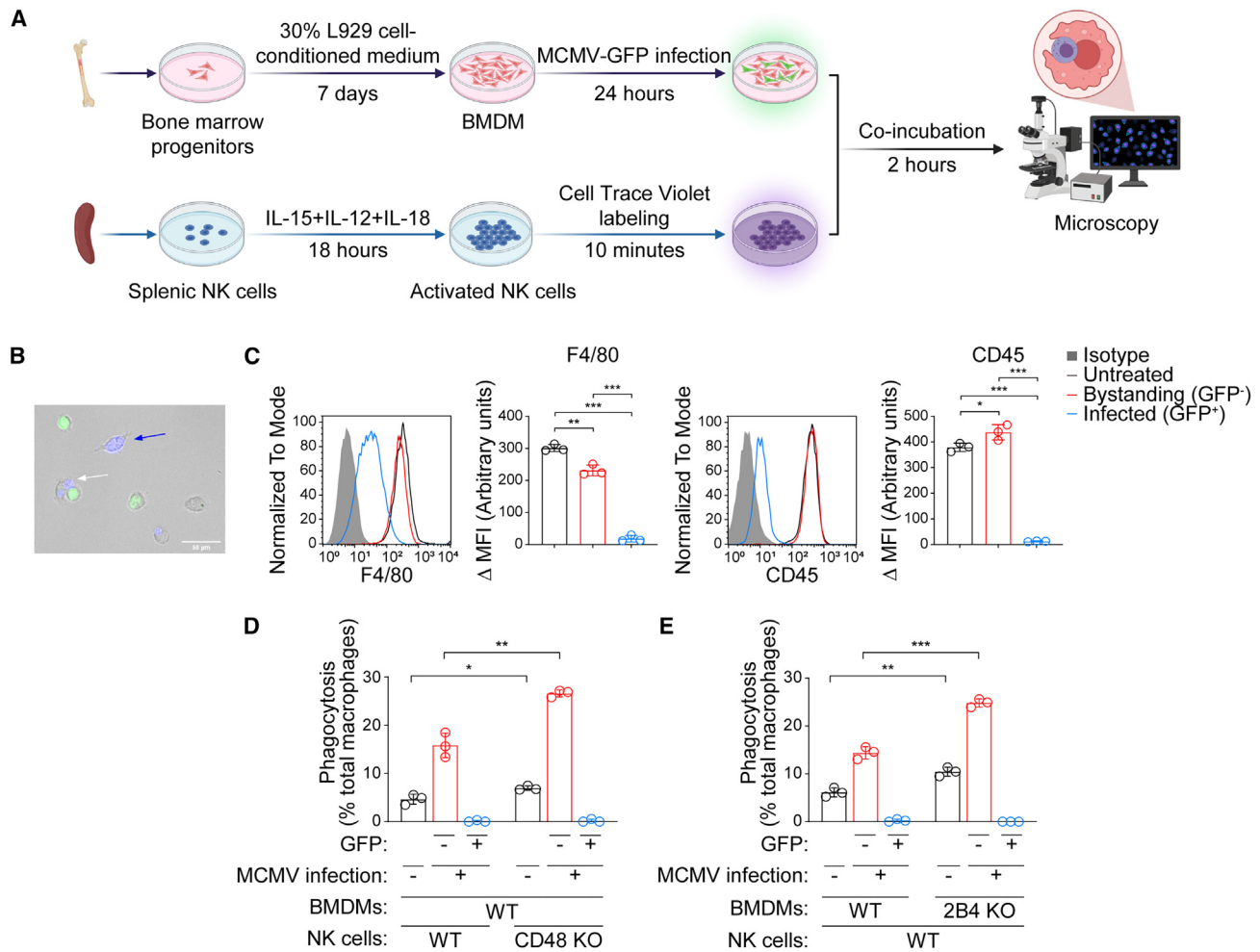


Figure 6. 2B4-CD48 axis inhibits phagocytosis of activated NK cells in response to MCMV infection

(A) Schematic diagram of the *in vitro* phagocytosis assay. BMDMs and NK cells were prepared under the indicated conditions. About 10% of the BMDMs were GFP⁺ (infected macrophages), and 90% of the BMDMs were GFP⁻ (bystanding macrophages). Phagocytosis assays were performed by co-incubating the macrophages and NK cells for 2 h followed by microscopic analysis to identify the phagocytosis rate of NK cells by macrophages.

(B) Representative merged microscopic picture showing the infected macrophage (GFP⁺), bystanding macrophage (GFP⁻), and NK cells (labeled with CellTrace violet) at the end of the phagocytosis assay. The blue arrow indicates an example of NK cells (violet) phagocytosed by a bystanding macrophage (gray). The white arrow indicates an example of an NK cell conjugated with a bystanding macrophage. This is not counted as a phagocytosis event. Scale bar, 50 μ m.

(C) Flow cytometry analysis and statistical analysis of the expression of F4/80 (left two graphs) and CD45 (right two graphs) on untreated macrophages (black), bystanding macrophages (red), and infected macrophages (blue). Isotype controls are shown in gray (n = 3).

(D) Statistical results of the phagocytosis assay using WT BMDMs as effector cells and WT or CD48 KO NK cells as target cells. The uninfected BMDMs were used as controls. The phagocytosis rates of bystanding macrophages (GFP⁻) and infected macrophages (GFP⁺) were counted and analyzed (n = 3).

(E) Same as (D), except that WT or 2B4 KO BMDMs were used as effector cells and WT NK cells were used as target cells (n = 3). Statistical analyses were conducted using one-way ANOVA followed by Tukey's multiple comparisons test. Each symbol represents an individual mouse; error bars depict the mean with SD. *p \leq 0.05, **p \leq 0.01, ***p \leq 0.001; ns, not significant. Data are representative of three independent experiments.

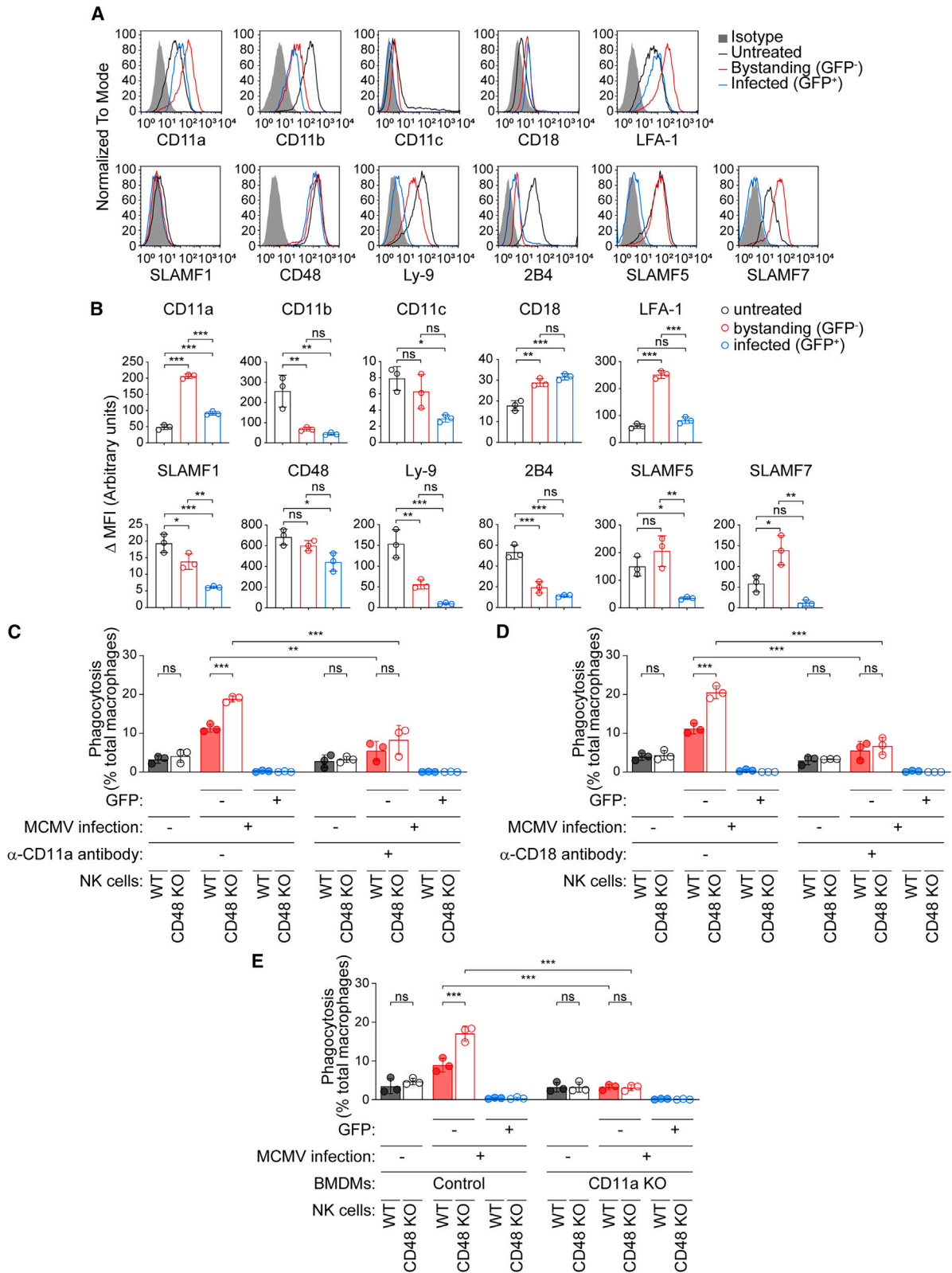
phagocytosis caused by loss of CD48 on NK cells was abrogated. Next, we examined the effect of genetic loss of CD11a in macrophages. Unlike wild-type BMDMs, CD11a KO BMDMs did not exhibit any increase in phagocytosis of CD48 KO NK cells compared with wild-type NK cells (Figure 7E).

Thus, the augmented phagocytosis of CD48 KO NK cells by bystanding macrophages was mediated by LFA-1 (CD11a-CD18). Given the impact of the blocking antibodies, it is likely

that LFA-1 recognized pro-phagocytic ligands on activated NK cells, as suggested elsewhere.⁴²

DISCUSSION

Here, we found that CD48 expressed on Ly49H⁺ NK cells was crucial for the expansion of adaptive Ly49H⁺ NK cells after MCMV infection. This requirement was not due to a cell-intrinsic



(legend on next page)

impact of CD48 on activation, proliferation, or apoptosis of Ly49H⁺ NK cells, as assessed by the expression of CD69, KLRG1, Ki67, and activated caspases. Rather, our data indicated that CD48 attenuated the suppression of, and thereby promoting, Ly49H⁺ NK cell expansion after MCMV infection. As mentioned earlier, a related role was reported for type I IFN signaling, although in these cases, the protective role of type I IFN signaling was NK cell intrinsic.¹⁷ Our report is the first indication of an NK cell-extrinsic role of receptor-mediated signaling in adaptive NK cell expansion.

The role of CD48 in promoting the expansion of adaptive Ly49H⁺ NK cells required expression of its counter-receptor, 2B4, in the host. Nevertheless, this function was not dependent on host NK cells, which express 2B4. It was also not reliant on host T cells, as demonstrated using RAG-1 KO mice. Rather, it was dependent at least in part on host macrophages, which are also 2B4 positive. In support of this idea, elimination of macrophages by anti-CSF-1R antibodies or clodronate rescued the expansion defect of CD48 KO Ly49H⁺ NK cells relative to wild-type Ly49H⁺ NK cells. This rescue was partial, however, likely because these macrophage-depletion agents are not fully effective at removing tissue macrophages.^{34,39,44} This is especially true for anti-CSF-1R antibodies.^{34,39} It is conceivable that the remaining macrophages were sufficient to eliminate an appreciable proportion of the activated Ly49H⁺ NK cells during MCMV infection. There is not necessarily a linear relationship between number of macrophages and total phagocytic capacity. Another scenario is that the remaining macrophages, and perhaps other myeloid cells expressing 2B4, including dendritic cells and neutrophils, were compensating for the macrophage loss and becoming more efficient sites of viral replication and NK cell activation.

Evidence for the involvement of macrophages was also provided by the *in vitro* model of MCMV infection. Using BMDMs infected by a GFP-encoding variant of MCMV, we observed that bystander macrophages, but not infected macrophages, exhibited greater phagocytosis of CD48 KO NK cells compared with wild-type NK cells. Likewise, compared with wild-type bystander BMDMs, 2B4 KO bystander BMDMs were more efficient at phagocytosis of wild-type NK cells.

One of the key roles of macrophages during infections is to eliminate pathogens, in addition to damaged and unwanted host cells, via phagocytosis.⁴⁵ Such a process is facilitated by

the attenuation of inhibitory signals in macrophages. In agreement with this concept, expression of 2B4 was decreased on bystander macrophages after MCMV infection. This modification likely favored the elimination of unwanted CD48-positive cells, including various immune cells. Paradoxically, adaptive Ly49H⁺ NK cells exhibited augmented expression of CD48 after MCMV infection. Augmented expression of CD48 on NK cells, in the face of decreasing expression of 2B4 on macrophages, may be aimed at selectively protecting activated Ly49H⁺ NK cells, but not unwanted immune cells, from phagocytosis.

In addition to reduced inhibitory signals, phagocytosis is dependent on the engagement of one or more activating receptors on macrophages by their ligands on target cells.^{46,47} Our data suggested that macrophage-expressed LFA-1, or CD11a-CD18, was critical for the enhanced phagocytosis of CD48 KO NK cells after MCMV infection. Future studies involving conditional KO mice in which expression of LFA-1 can be specifically eliminated in macrophages will be needed to confirm this requirement *in vivo*. We also observed that expression of CD11a, but not of related integrins CD11b and CD11c, on macrophages was augmented upon MCMV infection. The observation that 2B4 suppressed the function of LFA-1 in macrophages was reminiscent of our previous finding that, in mouse NK cells, 2B4 inhibited NK cell cytotoxicity by repressing the activity of LFA-1.²⁶ In NK cells, the inhibitory function of 2B4 was mediated by lipid phosphatase SHIP-1, which prevented inside-out activation of LFA-1. Whether a similar mechanism is operational in macrophages deserves consideration.

Within the SLAM family, the 2B4-CD48 axis played the most predominant role in the expansion of adaptive MCMV-specific NK cells. Although SLAMF7 also favored the expansion of Ly49H⁺ NK cells, its effect was much more modest. Given the previously reported role of SLAMF7 as an activating receptor in NK cells,⁴⁸ it is conceivable that SLAMF7 was cooperating with Ly49H and other receptors such as DNAM-1 to enable optimal NK cell activation in response to MCMV. Conversely, we found that NK cell-expressed 2B4 suppressed expansion of adaptive Ly49H⁺ NK cells. Considering that 2B4 has been shown to mediate inhibitory signals in mouse NK cells,^{23,26} it is plausible that this SFR acted by inhibiting NK cell activation in response to the virus.

In summary, we have identified a previously unsuspected mechanism involving macrophages that is critical for expansion

Figure 7. Integrin LFA-1 mediates phagocytosis of NK cells regulated by the 2B4-CD48 axis

(A) Flow cytometry analysis of the expression of β 2-integrins and SLAM family receptors on untreated macrophages (black), bystander macrophages (GFP⁻; red), and infected macrophages (GFP⁺; blue). Isotype controls are shown in gray.
 (B) Same as (A), except statistical analyses of the results are depicted (n = 3).
 (C) Phagocytosis assays with blocking antibody were performed by co-incubating the macrophages and NK cells for 2 h in the presence of anti-CD11a or isotype control antibody. WT BMDMs were used as effector cells and WT NK cells (filled columns) or CD48 KO NK cells (open columns) were used as target cells. The uninfected BMDMs were used as controls. The phagocytosis rates of bystander macrophages (GFP⁻) and infected macrophages (GFP⁺) are depicted (n = 3).
 (D) Same experiments as in (C), except that the results with anti-CD18 antibody and the respective isotype control are depicted (n = 3).
 (E) Phagocytosis assays were performed using BMDMs from CD11a-deficient mice or the CD11a-positive control mice as effector cells and WT NK cells (filled columns) or CD48 KO NK cells (open columns) as target cells. Either CD11a single-deficient mice (CD11a^{-/-}, Ly49H⁺) or CD11a-Ly49H double-deficient mice (CD11a^{-/-}, Ly49H^{-/-}) were used to generate CD11a KO BMDMs. WT (CD11a^{+/+}, Ly49H⁺) or Ly49H single-deficient (CD11a^{+/+}, Ly49H^{-/-}) BMDMs were used as controls. The uninfected BMDMs (black) were used as controls. Statistical results of the phagocytosis assay of bystander macrophages (GFP⁻) and infected macrophages (GFP⁺) are depicted (n = 3). Statistical analyses were conducted using one-way ANOVA followed by Tukey's multiple comparisons test. Each symbol represents an individual mouse; error bars depict the mean with SD. *p ≤ 0.05, **p ≤ 0.01, ***p ≤ 0.001; ns, not significant. Data are representative of three independent experiments.

of adaptive NK cells after MCMV infection. This mechanism involves CD48 on Ly49H⁺ NK cells and its counter-receptor 2B4 on host macrophages. When engaged by CD48, 2B4 suppresses the ability of bystanding macrophages, which are activated upon MCMV infection, to phagocytose and promotes the expansion of activated Ly49H⁺ NK cells following viral infection. This process likely accelerates elimination of virus-infected cells and, ultimately, facilitates the generation of a larger pool of long-lived adaptive NK cells.

In addition to augmenting our comprehension of the processes leading to expansion of adaptive NK cells, these data provide a first indication of the key role of macrophages in the homeostasis of adaptive NK cells. While previous data documented the involvement of macrophages in MCMV propagation, as well as in immune cell activation and viral clearance during MCMV infection,^{49–51} our findings show that macrophages also have the capacity to eliminate virus-activated NK cells and that this function needs to be suppressed by 2B4-CD48. It will be interesting to determine if a similar function exists after infection with other viruses, such as HCMV, or during the production of CIML NK cells in response to cytokines. It is also tempting to speculate that therapeutic stimulation of the 2B4-CD48 axis might enhance the generation of adaptive NK cells or CIML NK cells for clinical purposes toward the treatment of human diseases such as viral infections and cancer.

Limitations of the study

Future studies will be necessary to determine whether the effects of 2B4-CD48 observed *in vivo* were mediated solely by macrophages or whether other immune cell types were involved. Moreover, it remains to be clarified whether the 2B4-CD48 mechanism also exists for human virus-specific adaptive NK cells and CIML NK cells and whether our proposed mechanism involving 2B4-CD48 can be harnessed for therapeutic purposes in clinical settings. Last, our experiments on the role of LFA-1 were conducted only *in vitro*, because no conditional CD11a-deficient mouse strain is available. Appropriate *in vivo* studies will be needed to prove that LFA-1 was the activating receptor responsible for phagocytosis of NK cells during MCMV infection.

STAR★METHODS

Detailed methods are provided in the online version of this paper and include the following:

- **KEY RESOURCES TABLE**
- **RESOURCE AVAILABILITY**
 - Lead contact
 - Materials availability
 - Data and code availability
- **EXPERIMENTAL MODEL AND STUDY PARTICIPANT DETAILS**
 - Mice
- **METHOD DETAILS**
 - NK cell enrichment and adoptive transfer
 - *In vivo* MCMV infection and analyses of virus-specific NK cells
 - Flow cytometry

- *In vivo* macrophage depletion
- *In vitro* infection of macrophages with MCMV
- Microscopy-based phagocytosis assay
- **QUANTIFICATION AND STATISTICAL ANALYSIS**

SUPPLEMENTAL INFORMATION

Supplemental information can be found online at <https://doi.org/10.1016/j.celrep.2024.113800>.

ACKNOWLEDGMENTS

We thank members of the Veillette laboratory for useful discussions. We thank Dominique Gütle for her technical help during the MCMV-GFP virus preparation. The cartoons were generated using Biorender.com. This work was supported by grants from the Canadian Institutes of Health Research (MT-14429, MOP-82906, FDN-143338, PJT-178314 and PJT-183593) and the International Development Research Centre (Project 108403) to A.V. and from the Natural Sciences and Engineering Research Council of Canada (RGPIN-06457) and Genome Canada and Ontario Genomics (OGI-137) to S.M.V. R.L. was the recipient of a Lloyd Carr-Harris fellowship. A.V. holds the Canada Research Chair on Signaling in the Immune System.

AUTHOR CONTRIBUTIONS

Conceptualization, A.V. and J.C.S.; methodology, A.V., J.C.S., S.M.V., Z.R., R.L., C.C.G., and D.D.; investigation, A.V., R.L., C.C.G., and D.D.; visualization, A.V., R.L., C.C.G., and D.D.; funding acquisition, A.V., S.M.V., and R.L.; project administration, A.V.; supervision, A.V., J.C.S., and S.M.V.; writing – original draft, A.V., R.L., C.C.G., and D.D.; writing – review & editing, A.V., R.L., C.C.G., D.D., J.C.S., S.M.V., H.G., M.-C.Z., J.Q., B.L., Z.R., C.M.L., and T.E.O.

DECLARATION OF INTERESTS

The authors declare no competing interests.

Received: June 30, 2023

Revised: December 21, 2023

Accepted: January 31, 2024

REFERENCES

1. Demaria, O., Cornen, S., Daëron, M., Morel, Y., Medzhitov, R., and Vivier, E. (2019). Harnessing innate immunity in cancer therapy. *Nature* 574, 45–56. <https://doi.org/10.1038/s41586-019-1593-5>.
2. Diefenbach, A., and Raulet, D.H. (2003). Innate immune recognition by stimulatory immunoreceptors. *Curr. Opin. Immunol.* 15, 37–44. [https://doi.org/10.1016/s0952-7915\(02\)00007-9](https://doi.org/10.1016/s0952-7915(02)00007-9).
3. Daëron, M., Jaeger, S., Du Pasquier, L., and Vivier, E. (2008). Immunoreceptor tyrosine-based inhibition motifs: a quest in the past and future. *Immunol. Rev.* 224, 11–43. <https://doi.org/10.1111/j.1600-065X.2008.00666.x>.
4. Gang, M., Wong, P., Berrien-Elliott, M.M., and Fehniger, T.A. (2020). Memory-like natural killer cells for cancer immunotherapy. *Semin. Hematol.* 57, 185–193. <https://doi.org/10.1053/j.seminhematol.2020.11.003>.
5. Fehniger, T.A., and Cooper, M.A. (2016). Harnessing NK Cell Memory for Cancer Immunotherapy. *Trends Immunol.* 37, 877–888. <https://doi.org/10.1016/j.it.2016.09.005>.
6. Berrien-Elliott, M.M., Wagner, J.A., and Fehniger, T.A. (2015). Human Cytokine-Induced Memory-Like Natural Killer Cells. *J. Innate Immun.* 7, 563–571. <https://doi.org/10.1159/000382019>.
7. Paust, S., Gill, H.S., Wang, B.Z., Flynn, M.P., Moseman, E.A., Senman, B., Szczepaniak, M., Telenti, A., Askenase, P.W., Compans, R.W., and von Andrian, U.H. (2010). Critical role for the chemokine receptor CXCR6 in NK

- cell-mediated antigen-specific memory of haptens and viruses. *Nat. Immunol.* **11**, 1127–1135. <https://doi.org/10.1038/ni.1953>.
8. Sheppard, S., and Sun, J.C. (2021). Virus-specific NK cell memory. *J. Exp. Med.* **218**, e20201731. <https://doi.org/10.1084/jem.20201731>.
 9. O'Sullivan, T.E., Sun, J.C., and Lanier, L.L. (2015). Natural Killer Cell Memory. *Immunity* **43**, 634–645. <https://doi.org/10.1016/j.immuni.2015.09.013>.
 10. Schlums, H., Cichocki, F., Tesi, B., Theorell, J., Beziat, V., Holmes, T.D., Han, H., Chiang, S.C.C., Foley, B., Mattsson, K., et al. (2015). Cytomegalovirus infection drives adaptive epigenetic diversification of NK cells with altered signaling and effector function. *Immunity* **42**, 443–456. <https://doi.org/10.1016/j.immuni.2015.02.008>.
 11. Sun, J.C., Beilke, J.N., and Lanier, L.L. (2009). Adaptive immune features of natural killer cells. *Nature* **457**, 557–561. <https://doi.org/10.1038/nature07665>.
 12. Cerwenka, A., and Lanier, L.L. (2016). Natural killer cell memory in infection, inflammation and cancer. *Nat. Rev. Immunol.* **16**, 112–123. <https://doi.org/10.1038/nri.2015.9>.
 13. Nabekura, T., Kanaya, M., Shibuya, A., Fu, G., Gascoigne, N.R.J., and Lanier, L.L. (2014). Costimulatory molecule DNAM-1 is essential for optimal differentiation of memory natural killer cells during mouse cytomegalovirus infection. *Immunity* **40**, 225–234. <https://doi.org/10.1016/j.immuni.2013.12.011>.
 14. Sun, J.C., Madera, S., Bezman, N.A., Beilke, J.N., Kaplan, M.H., and Lanier, L.L. (2012). Proinflammatory cytokine signaling required for the generation of natural killer cell memory. *J. Exp. Med.* **209**, 947–954. <https://doi.org/10.1084/jem.20111760>.
 15. Madera, S., and Sun, J.C. (2015). Cutting edge: stage-specific requirement of IL-18 for antiviral NK cell expansion. *J. Immunol.* **194**, 1408–1412. <https://doi.org/10.4049/jimmunol.1402001>.
 16. Lau, C.M., Adams, N.M., Geary, C.D., Weizman, O.E., Rapp, M., Pritykin, Y., Leslie, C.S., and Sun, J.C. (2018). Epigenetic control of innate and adaptive immune memory. *Nat. Immunol.* **19**, 963–972. <https://doi.org/10.1038/s41590-018-0176-1>.
 17. Madera, S., Rapp, M., Firth, M.A., Beilke, J.N., Lanier, L.L., and Sun, J.C. (2016). Type I IFN promotes NK cell expansion during viral infection by protecting NK cells against fratricide. *J. Exp. Med.* **213**, 225–233. <https://doi.org/10.1084/jem.20150712>.
 18. Min-Oo, G., Bezman, N.A., Madera, S., Sun, J.C., and Lanier, L.L. (2014). Proapoptotic Bim regulates antigen-specific NK cell contraction and the generation of the memory NK cell pool after cytomegalovirus infection. *J. Exp. Med.* **211**, 1289–1296. <https://doi.org/10.1084/jem.20132459>.
 19. Wu, N., and Veillette, A. (2016). SLAM family receptors in normal immunity and immune pathologies. *Curr. Opin. Immunol.* **38**, 45–51. <https://doi.org/10.1016/j.coi.2015.11.003>.
 20. Veillette, A., and Guo, H. (2013). CS1, a SLAM family receptor involved in immune regulation, is a therapeutic target in multiple myeloma. *Crit. Rev. Oncol. Hematol.* **88**, 168–177. <https://doi.org/10.1016/j.critrevonc.2013.04.003>.
 21. Veillette, A. (2010). SLAM-family receptors: immune regulators with or without SAP-family adaptors. *Cold Spring Harb. Perspect. Biol.* **2**, a002469. <https://doi.org/10.1101/cshperspect.a002469>.
 22. Cannons, J.L., Tangye, S.G., and Schwartzberg, P.L. (2011). SLAM family receptors and SAP adaptors in immunity. *Annu. Rev. Immunol.* **29**, 665–705. <https://doi.org/10.1146/annurev-immunol-030409-101302>.
 23. Wu, N., Zhong, M.C., Roncagalli, R., Pérez-Quintero, L.A., Guo, H., Zhang, Z., Lenoir, C., Dong, Z., Latour, S., and Veillette, A. (2016). A hematopoietic cell-driven mechanism involving SLAMF6 receptor, SAP adaptors and SHP-1 phosphatase regulates NK cell education. *Nat. Immunol.* **17**, 387–396. <https://doi.org/10.1038/ni.3369>.
 24. Chen, S., Yang, M., Du, J., Li, D., Li, Z., Cai, C., Ma, Y., Zhang, L., Tian, Z., and Dong, Z. (2016). The Self-Specific Activation Receptor SLAM Family Is Critical for NK Cell Education. *Immunity* **45**, 292–304. <https://doi.org/10.1016/j.immuni.2016.07.013>.
 25. Beaulieu, A.M., Zawislak, C.L., Nakayama, T., and Sun, J.C. (2014). The transcription factor Zbtb32 controls the proliferative burst of virus-specific natural killer cells responding to infection. *Nat. Immunol.* **15**, 546–553. <https://doi.org/10.1038/ni.2876>.
 26. Guo, H., Cranert, S.A., Lu, Y., Zhong, M.C., Zhang, S., Chen, J., Li, R., Mahl, S.E., Wu, N., Davidson, D., et al. (2016). Deletion of Slam locus in mice reveals inhibitory role of SLAM family in NK cell responses regulated by cytokines and LFA-1. *J. Exp. Med.* **213**, 2187–2207. <https://doi.org/10.1084/jem.20160552>.
 27. Sun, J.C., Lopez-Verges, S., Kim, C.C., DeRisi, J.L., and Lanier, L.L. (2011). NK cells and immune "memory". *J. Immunol.* **186**, 1891–1897. <https://doi.org/10.4049/jimmunol.1003035>.
 28. Sun, J.C., Beilke, J.N., and Lanier, L.L. (2010). Immune memory redefined: characterizing the longevity of natural killer cells. *Immunol. Rev.* **236**, 83–94. <https://doi.org/10.1111/j.1600-065X.2010.00900.x>.
 29. McArdel, S.L., Terhorst, C., and Sharpe, A.H. (2016). Roles of CD48 in regulating immunity and tolerance. *Clin. Immunol.* **164**, 10–20. <https://doi.org/10.1016/j.clim.2016.01.008>.
 30. Gerdes, J., Schwab, U., Lemke, H., and Stein, H. (1983). Production of a mouse monoclonal antibody reactive with a human nuclear antigen associated with cell proliferation. *Int. J. Cancer* **31**, 13–20. <https://doi.org/10.1002/ijc.2910310104>.
 31. Fogel, L.A., Sun, M.M., Geurs, T.L., Carayannopoulos, L.N., and French, A.R. (2013). Markers of nonselective and specific NK cell activation. *J. Immunol.* **190**, 6269–6276. <https://doi.org/10.4049/jimmunol.1202533>.
 32. Chiossone, L., Chaix, J., Fuseri, N., Roth, C., Vivier, E., and Walzer, T. (2009). Maturation of mouse NK cells is a 4-stage developmental program. *Blood* **113**, 5488–5496. <https://doi.org/10.1182/blood-2008-10-187179>.
 33. Julien, O., and Wells, J.A. (2017). Caspases and their substrates. *Cell Death Differ.* **24**, 1380–1389. <https://doi.org/10.1038/cdd.2017.44>.
 34. Li, D., Xiong, W., Wang, Y., Feng, J., He, Y., Du, J., Wang, J., Yang, M., Zeng, H., Yang, Y.G., et al. (2022). SLAMF3 and SLAMF4 are immune checkpoints that constrain macrophage phagocytosis of hematopoietic tumors. *Sci. Immunol.* **7**, eabj5501. <https://doi.org/10.1126/sciimmunol.abj5501>.
 35. Taniguchi, R.T., Guziar, D., and Kumar, V. (2007). 2B4 inhibits NK-cell fratricide. *Blood* **110**, 2020–2023. <https://doi.org/10.1182/blood-2007-02-076927>.
 36. Cao, X., Shores, E.W., Hu-Li, J., Anver, M.R., Kelsall, B.L., Russell, S.M., Drago, J., Noguchi, M., Grinberg, A., Bloom, E.T., et al. (1995). Defective lymphoid development in mice lacking expression of the common cytokine receptor gamma chain. *Immunity* **2**, 223–238. [https://doi.org/10.1016/1074-7613\(95\)90047-0](https://doi.org/10.1016/1074-7613(95)90047-0).
 37. Shinkai, Y., Rathbun, G., Lam, K.P., Oltz, E.M., Stewart, V., Mendelsohn, M., Charron, J., Datta, M., Young, F., Stall, A.M., et al. (1992). RAG-2-deficient mice lack mature lymphocytes owing to inability to initiate V(D)J recombination. *Cell* **68**, 855–867. [https://doi.org/10.1016/0092-8674\(92\)90029-c](https://doi.org/10.1016/0092-8674(92)90029-c).
 38. Karo, J.M., Schatz, D.G., and Sun, J.C. (2014). The RAG recombinase dictates functional heterogeneity and cellular fitness in natural killer cells. *Cell* **159**, 94–107. <https://doi.org/10.1016/j.cell.2014.08.026>.
 39. Tagliani, E., Shi, C., Nancy, P., Tay, C.S., Pamer, E.G., and Erlebacher, A. (2011). Coordinate regulation of tissue macrophage and dendritic cell population dynamics by CSF-1. *J. Exp. Med.* **208**, 1901–1916. <https://doi.org/10.1084/jem.20110866>.
 40. van Rooijen, N., van Nieuwmegen, R., and Kamperdijk, E.W. (1985). Elimination of phagocytic cells in the spleen after intravenous injection of liposome-encapsulated dichloromethylene diphosphonate. Ultrastructural aspects of elimination of marginal zone macrophages. *Virchows Arch. B Cell Pathol. Incl. Mol. Pathol.* **49**, 375–383. <https://doi.org/10.1007/BF02912114>.

41. Baasch, S., Giansanti, P., Kolter, J., Riedl, A., Forde, A.J., Runge, S., Zenke, S., Elling, R., Halenius, A., Brabletz, S., et al. (2021). Cytomegalovirus subverts macrophage identity. *Cell* 184, 3774–3793.e25. <https://doi.org/10.1016/j.cell.2021.05.009>.
42. Tang, Z., Davidson, D., Li, R., Zhong, M.C., Qian, J., Chen, J., and Veillette, A. (2021). Inflammatory macrophages exploit unconventional pro-phagocytic integrins for phagocytosis and anti-tumor immunity. *Cell Rep.* 37, 110111. <https://doi.org/10.1016/j.celrep.2021.110111>.
43. Hynes, R.O. (2002). Integrins: bidirectional, allosteric signaling machines. *Cell* 110, 673–687. [https://doi.org/10.1016/s0092-8674\(02\)00971-6](https://doi.org/10.1016/s0092-8674(02)00971-6).
44. van Rooijen, N., and Sanders, A. (1997). Elimination, blocking, and activation of macrophages: three of a kind? *J. Leukoc. Biol.* 62, 702–709. <https://doi.org/10.1002/jlb.62.6.702>.
45. Hirayama, D., Iida, T., and Nakase, H. (2017). The Phagocytic Function of Macrophage-Enforcing Innate Immunity and Tissue Homeostasis. *Int. J. Mol. Sci.* 19, 92. <https://doi.org/10.3390/ijms19010092>.
46. Shaw, D.R., and Griffin, F.M., Jr. (1981). Phagocytosis requires repeated triggering of macrophage phagocytic receptors during particle ingestion. *Nature* 289, 409–411. <https://doi.org/10.1038/289409a0>.
47. Aderem, A., and Underhill, D.M. (1999). Mechanisms of phagocytosis in macrophages. *Annu. Rev. Immunol.* 17, 593–623. <https://doi.org/10.1146/annurev.immunol.17.1.593>.
48. Cruz-Munoz, M.E., Dong, Z., Shi, X., Zhang, S., and Veillette, A. (2009). Influence of CRACC, a SLAM family receptor coupled to the adaptor EAT-2, on natural killer cell function. *Nat. Immunol.* 10, 297–305. <https://doi.org/10.1038/ni.1693>.
49. Hokeness, K.L., Kuziel, W.A., Biron, C.A., and Salazar-Mather, T.P. (2005). Monocyte chemoattractant protein-1 and CCR2 interactions are required for IFN-alpha/beta-induced inflammatory responses and antiviral defense in liver. *J. Immunol.* 174, 1549–1556. <https://doi.org/10.4049/jimmunol.174.3.1549>.
50. Salazar-Mather, T.P., Lewis, C.A., and Biron, C.A. (2002). Type I interferons regulate inflammatory cell trafficking and macrophage inflammatory protein 1alpha delivery to the liver. *J. Clin. Invest.* 110, 321–330. <https://doi.org/10.1172/JCI115376>.
51. Hanson, L.K., Slater, J.S., Karabekian, Z., Virgin, H.W., 4th, Biron, C.A., Ruzek, M.C., van Rooijen, N., Ciavarra, R.P., Stenberg, R.M., and Campbell, A.E. (1999). Replication of murine cytomegalovirus in differentiated macrophages as a determinant of viral pathogenesis. *J. Virol.* 73, 5970–5980. <https://doi.org/10.1128/JVI.73.7.5970-5980.1999>.
52. Fodil-Cornu, N., Lee, S.H., Belanger, S., Makrigiannis, A.P., Biron, C.A., Buller, R.M., and Vidal, S.M. (2008). Ly49h-deficient C57BL/6 mice: a new mouse cytomegalovirus-susceptible model remains resistant to unrelated pathogens controlled by the NK gene complex. *J. Immunol.* 181, 6394–6405. <https://doi.org/10.4049/jimmunol.181.9.6394>.
53. Chen, J., Zhong, M.C., Guo, H., Davidson, D., Mishel, S., Lu, Y., Rhee, I., Pérez-Quintero, L.A., Zhang, S., Cruz-Munoz, M.E., et al. (2017). SLAMF7 is critical for phagocytosis of haematopoietic tumour cells via Mac-1 integrin. *Nature* 544, 493–497. <https://doi.org/10.1038/nature22076>.
54. Lu, Y., Zhong, M.C., Qian, J., Calderon, V., Cruz Tleugabulova, M., Mallevaey, T., and Veillette, A. (2019). SLAM receptors foster iNKT cell development by reducing TCR signal strength after positive selection. *Nat. Immunol.* 20, 447–457. <https://doi.org/10.1038/s41590-019-0334-0>.
55. Zhong, M.C., Lu, Y., Qian, J., Zhu, Y., Dong, L., Zahn, A., Di Noia, J.M., Karo-Atar, D., King, I.L., and Veillette, A. (2021). SLAM family receptors control pro-survival effectors in germinal center B cells to promote humoral immunity. *J. Exp. Med.* 218, e20200756. <https://doi.org/10.1084/jem.20200756>.
56. Li, B., Lu, Y., Zhong, M.C., Qian, J., Li, R., Davidson, D., Tang, Z., Zhu, K., Argenty, J., de Peredo, A.G., et al. (2022). Cis interactions between CD2 and its ligands on T cells are required for T cell activation. *Sci. Immunol.* 7, eabn6373. <https://doi.org/10.1126/sciimmunol.abn6373>.
57. O'Sullivan, T.E., Johnson, L.R., Kang, H.H., and Sun, J.C. (2015). BNIP3- and BNIP3L-Mediated Mitophagy Promotes the Generation of Natural Killer Cell Memory. *Immunity* 43, 331–342. <https://doi.org/10.1016/j.immuni.2015.07.012>.
58. Fodil, N., Langlais, D., Moussa, P., Boivin, G.A., Di Pietrantonio, T., Radovanovic, I., Dumaine, A., Blanchette, M., Schurr, E., Gros, P., and Vidal, S.M. (2014). Specific dysregulation of IFNgamma production by natural killer cells confers susceptibility to viral infection. *PLoS Pathog.* 10, e1004511. <https://doi.org/10.1371/journal.ppat.1004511>.
59. Rhee, I., Davidson, D., Souza, C.M., Vacher, J., and Veillette, A. (2013). Macrophage fusion is controlled by the cytoplasmic protein tyrosine phosphatase PTP-PEST/PTPN12. *Mol. Cell Biol.* 33, 2458–2469. <https://doi.org/10.1128/MCB.00197-13>.

STAR★METHODS

KEY RESOURCES TABLE

REAGENT or RESOURCE	SOURCE	IDENTIFIER
Antibodies		
Anti-mouse 2B4-PE (m2B4 (B6) 458.1)	BioLegend	Cat#133508; RRID: AB_2072855
Anti-mouse CD11a-PE (M17/4)	BioLegend	Cat#101107; RRID: AB_312780
Anti-mouse CD11b-Pacific Blue (M1/70)	BioLegend	Cat#101224; RRID: AB_755986
Anti-mouse CD11b-PE/Cyanine7 (M1/70)	BioLegend	Cat#101216; RRID: AB_312799
Anti-mouse CD11c-PE (N418)	BioLegend	Cat#117308; RRID: AB_313777
Anti-mouse CD122-PE (TM-b1)	eBioscience	Cat#12-1222-83; RRID: AB_465837
Anti-mouse CD18-PE (M18/2)	BioLegend	Cat#101408; RRID: AB_312817
Anti-mouse CD27-PE (LG.7F9)	eBioscience	Cat#12-0271-82; RRID: AB_465614
Anti-mouse CD2-PE (RM2-5)	BioLegend	Cat#100108; RRID: AB_2073690
Anti-mouse CD3e-FITC (145-2C11)	BioLegend	Cat#100306; RRID: AB_312671
Anti-mouse CD3e-Pacific Blue (145-2C11)	BioLegend	Cat#100334; RRID: AB_2028475
Anti-mouse CD45.1-PE (A20)	BioLegend	Cat#110708; RRID: AB_313497
Anti-mouse CD45.2-FITC (104)	BioLegend	Cat#109806; RRID: AB_313443
Anti-mouse CD45-PE (30-F11)	BD Biosciences	Cat#553081; RRID: AB_394611
Anti-mouse CD48-FITC (HM48-1)	BioLegend	Cat#103404; RRID: AB_313019
Anti-mouse CD48-PE (HM48-1)	BioLegend	Cat#103406; RRID: AB_313021
Anti-mouse CD49b-APC (DX5)	BioLegend	Cat#108910; RRID: AB_313417
Anti-mouse CD69-APC (H1.2F3)	BioLegend	Cat#104514; RRID: AB_492843
Anti-mouse CD84-PE (mCD84.7)	BioLegend	Cat#122806; RRID: AB_2074756
Anti-mouse DNAM-1-APC (10E5)	BioLegend	Cat#128810; RRID: AB_2566627
Anti-mouse F4/80-APC (BM8)	BioLegend	Cat#123116; RRID: AB_893481
Anti-mouse ICAM-1 (CD54)-PE (YN1/1.7.4)	BioLegend	Cat#116108; RRID: AB_313699
Anti-mouse ICAM-2 (CD102)- Alexa Fluor 647 (3C4 (MIC2/4))	BioLegend	Cat#105612; RRID: AB_2122182
Anti-mouse Ki67-APC (16A8)	BioLegend	Cat#652406; RRID: AB_2561930
Anti-mouse KLRG1-APC (2F1/KLRG1)	BioLegend	Cat#138412; RRID: AB_10641560
Anti-mouse Ly49C/I/F/H-FITC (14B11)	eBioscience	Cat#11-5991-81; RRID: AB_465339
Anti-mouse Ly49D-FITC (4E5)	BioLegend	Cat#138303; RRID: AB_10588709
Anti-mouse Ly49G2-FITC (4D11)	eBioscience	Cat#11-5781-82; RRID: AB_763604
Anti-mouse Ly49H-APC (3D10)	BioLegend	Cat#144712; RRID: AB_2783111
Anti-mouse Ly49H-FITC (3D10)	BioLegend	Cat#144708; RRID: AB_2561744
Anti-mouse Ly-9-APC (Ly9ab3)	BioLegend	Cat# 122907; RRID: AB_2561312
Anti-mouse NK1.1-PE/Cyanine7 (PK136)	BioLegend	Cat#108714; RRID: AB_389364
Anti-mouse NKG2A/C/E-FITC (20d5)	eBioscience	Cat#11-5896-82; RRID: AB_465305
Anti-mouse NKG2D-PE (CX5)	BioLegend	Cat#130208; RRID: AB_1227712
Anti-mouse NKp46-PE (29A1.4)	BioLegend	Cat#137604; RRID: AB_2235755
Anti-mouse SLAMF6 (Ly108)-PE (330-AJ)	BioLegend	Cat#134606; RRID: AB_2188095
Anti-mouse SLAMF7 (CD319)-PE (4G2)	BioLegend	Cat#152006; RRID: AB_2632677
Anti-mouse SLAM-PE (TC15-12F12.2)	BioLegend	Cat#115904; RRID: AB_313683
Anti-mouse TCR-β- PE/Cyanine5 (H57-597)	BioLegend	Cat#109210; RRID: AB_313433
Anti-mouse TCR-β-FITC (H57-597)	BioLegend	Cat#109206; RRID: AB_313429
Anti-mouse TCR-β-Pacific Blue (H57-597)	BioLegend	Cat#109226; RRID: AB_1027649
Armenian hamster IgG isotype control antibody-APC (HTK888)	BioLegend	Cat#400912

(Continued on next page)

Continued

REAGENT or RESOURCE	SOURCE	IDENTIFIER
Armenian hamster IgG isotype control antibody-FITC (HTK888)	BioLegend	Cat#400906
Armenian hamster IgG isotype control antibody-PE (HTK888)	BioLegend	Cat#400907; RRID: AB_326593
Mouse IgG1 κ isotype control antibody-PE (MOPC-21)	BioLegend	Cat#400112; RRID: AB_2847829
Mouse IgG2a κ isotype control antibody-PE (MOPC-173)	BioLegend	Cat#400212; RRID: AB_326460
Rat IgG1 κ isotype control antibody-APC (RTK2071)	BioLegend	Cat#400412; RRID: AB_326518
Rat IgG1 κ isotype control antibody-PE (RTK2071)	BioLegend	Cat#400408; RRID: AB_326514
Rat IgG2a κ isotype control antibody-Alexa Fluor 647 (RTK2758)	BioLegend	Cat#400526; RRID: AB_2864284
Rat IgG2a κ isotype control antibody-APC (RTK2758)	BioLegend	Cat#400512; RRID: AB_2814702
Rat IgG2a κ isotype control antibody-FITC (RTK2758)	BioLegend	Cat#400506; RRID: AB_2736919
Rat IgG2a κ isotype control antibody-PE (RTK2758)	BioLegend	Cat#400508; RRID: AB_326530
Rat IgG2b κ isotype control antibody- PE/ Cyanine7 (RTK4530)	BioLegend	Cat#400618; RRID: AB_326560
Rat IgG2b κ isotype control antibody-APC (RTK4530)	BioLegend	Cat#400612; RRID: AB_326556
Rat IgG2b κ isotype control antibody- Pacific Blue (RTK4530)	BioLegend	Cat#400527; RRID: AB_2864285
Rat IgG2b κ isotype control antibody-PE (RTK4530)	BioLegend	Cat#400608; RRID: AB_326552
Anti-mouse CSF1R (AFS98)	Bio X Cell	Cat#BE0213; RRID: AB_2687699
Rat IgG2a κ isotype control (2A3)	Bio X Cell	Cat#BE0089; RRID: AB_1107769
Anti-mouse CD11a (M17/4)	eBioscience	Cat#16-0111-82; RRID:AB_468881
Rat IgG2a κ isotype control (eBR2a)	eBioscience	Cat#16-4321-85; RRID:AB_470156
Anti-mouse CD18 (GAME-46)	BD Biosciences	Cat#555280; RRID: AB_395703
Rat IgG1 isotype control (R3-34)	BD Biosciences	Cat#553921; RRID: AB_395507
Anti-mouse CD16/32 (2.4G2) hybridoma supernatant	In house	N/A
Anti-mouse CD25 (7G7) hybridoma supernatant	In house	N/A
Bacterial and virus strains		
Murine Cytomegalovirus (MCMV)	The Center for Phenogenomics, Montreal	Smith strain
MCMV-GFP	Baasch et al., 2021 ⁴¹	N/A
Chemicals, peptides, and recombinant proteins		
RPMI-1640	Thermo Fisher Scientific	Cat#21870076
L929 cell-conditioned medium	In house	N/A
Recombinant Murine IL-15	PeptoTech	Cat#210-15
Recombinant Murine IL-12	PeptoTech	Cat#210-12
Recombinant Mouse IL-18	Bio-techne	Cat#B004-5
Clodronate liposomes & control liposomes	LIPOSOMA	Cat#CP-010-010

(Continued on next page)

REAGENT or RESOURCE	SOURCE	IDENTIFIER
Continued		
Critical commercial assays		
CaspGLOW™ Fluorescein Active Caspase Staining Kit	BioVision	Cat#K180-100
Foxp3/Transcription Factor Staining Buffer Set	ThermoFisher Scientific	Cat#00-5523-00
Fixation/Permeabilization Kit	BD Biosciences	Cat#554714
EasySep™ Mouse NK Cell Isolation Kit	STEMCELL Technologies	Cat#19855
EasySep™ magnet	STEMCELL Technologies	Cat#18000
CellTrace™ Violet (CTV) Cell Proliferation Kit	ThermoFisher Scientific	Cat#C34557
Zombie Violet Fixable Viability Kit	BioLegend	Cat#423113
Experimental models: Organisms/strains		
C57BL/6J	The Jackson Lab	Strain #: 000664; RRID:IMSR_JAX:000664
B6.SJL- <i>Ptprc^a Pepc^b</i> /BoyJ	The Jackson Lab	Strain #: 002014; RRID:IMSR_JAX:002014
SFR KO (B6-Del(1 <i>Cd244a-Slamf6</i>) ^{1<i>Ve</i>i})	In house	N/A
SLAMF1,5,6 tKO (B6- <i>Slamf1^{em1<i>Ve</i>i}Cd84^{em1<i>Ve</i>i}Slamf6^{em1<i>Ve</i>i}</i>)	In house	N/A
SLAMF1 KO (B6- <i>Slamf1^{em1<i>Ve</i>i}</i>)	In house	N/A
SLAMF6 KO (B6- <i>Slamf6^{tm1<i>Plis</i>/J}</i>)	The Jackson Lab	Strain #:024669; RRID:IMSR_JAX:024669
2B4 KO (B6- <i>Cd244a^{tm1<i>Ve</i>i}</i>)	In house	N/A
CD48 KO (B6- <i>Cd48^{em2<i>Ve</i>i}</i> , clone T6)	In house	N/A
CD48 KO (B6- <i>Cd48^{em3<i>Ve</i>i}</i> , clone T87)	In house	N/A
SLAMF7 KO (B6- <i>Slamf7^{tm1.1<i>Ve</i>i}</i>)	In house	N/A
CD2 KO (B6- <i>Cd2^{em2<i>Ve</i>i}</i>)	In house	N/A
Ly49H KO (B6.BXD8- <i>Klra8^{Cmv1-del1}</i>)	Fodil-Cornu et al., 2008 ⁵²	N/A
CD11a KO (B6.129S7- <i>Itga1^{tm1<i>Bll</i>/J}</i>)	The Jackson Lab	Strain #:005257; RRID:IMSR_JAX:005257
RAG-1 KO (B6.129S7- <i>Rag1^{tm1<i>Mom</i>/J}</i>)	The Jackson Lab	Strain #: 002216; RRID:IMSR_JAX:002216
RAG-2-IL-2R γ DKO (C57BL/6NTac.Cg- <i>Rag2^{tm1<i>Fwa</i>}Il2rg^{tm1<i>Wj</i>j}</i>)	Taconic	Model #: 4111-F; RRID:IMSR_TAC:4111
2B4-Ly49H DKO	This paper	N/A
CD2-Ly49H DKO	This paper	N/A
CD11a-Ly49H DKO	This paper	N/A
RAG-1-Ly49H DKO	This paper	N/A
Software and algorithms		
FlowJo 10.4	FlowJo	https://www.flowjo.com/
GraphPad Prism 8.0.2	GraphPad Software	https://www.graphpad.com/
Microsoft 365	Microsoft	https://www.microsoft.com/en-ca/
ImageJ	Schneider et al. 2012	https://imagej.nih.gov/ij/download.html/

RESOURCE AVAILABILITY

Lead contact

André Veillette (andre.veillette@ircm.qc.ca).

Materials availability

Further information and requests for resources and reagents should be directed to and will be fulfilled by the [lead contact](#).

Data and code availability

- All data reported in this paper will be shared by the [lead contact](#) upon reasonable request.
- This study did not generate new data or code.
- Any additional information required to reanalyze the data reported in this work paper is available from the [lead contact](#) upon reasonable request.

EXPERIMENTAL MODEL AND STUDY PARTICIPANT DETAILS

Mice

Mice lacking all SFRs (SFR KO), individual SFRs (including SLAMF1 KO, 2B4 KO, SLAMF6 KO, and SLAMF7 KO), the ligand CD48 (CD48 KO), or CD2 (CD2 KO) have been described elsewhere.^{23,26,42,53–56} To exclude the possibility of the phenotype being attributed to off-target effects of CRISPR-Cas, two clones of CD48 KO mice were used in this study: one with a 10-nucleotide deletion (clone T6) and another with a 1-nucleotide deletion (clone T87) in exon 2 of the CD48-encoding gene, *Slamf2*.⁵⁶ Both clones exhibited the same phenotype in the experiments conducted. Ly49H KO mice were generated by the laboratory of Dr. Silvia Vidal at McGill University, Montreal, Canada.⁵² C57BL/6J mice, B6.SJL (CD45.1) mice, RAG-1 KO mice and CD11a KO were obtained from The Jackson Laboratory. RAG-2-IL-2R γ DKO mice were purchased from Taconic Biosciences. 2B4-Ly49H DKO, CD2-Ly49H DKO, RAG-1-Ly49H DKO and CD11a-Ly49H DKO were generated by breeding the 2B4 KO, CD2 KO, RAG-1 KO or CD11a KO mice with Ly49H KO mice until double-deficient homozygosity was achieved. All mice were maintained in the C57BL/6J background, and kept in specific pathogen-free (SPF) animal facilities. Sex- and age-matched mice between 7 and 16 weeks of age were used for experiments. Littermates were used whenever possible, except for experiments involving B6.SJL mice. Experiments were performed using both male and female mice, with donors and recipients of the same sex being used in each individual experiment. Animal experiments were approved by the Animal Care Committee of the Institut de recherches cliniques de Montréal and performed as defined by the Canadian Council of Animal Care.

METHOD DETAILS

NK cell enrichment and adoptive transfer

NK cells were enriched from mouse splenocytes using the EasySepTM Mouse NK Cell Isolation Kit and EasySepTM magnet from STEMCELL Technologies. Enriched NK cells had purities ranging from 60% to 95%. Adoptive transfer experiments were performed as described.⁵⁷ In brief, for the competitive adoptive transfer assays, the proportion of Ly49H⁺ NK cells in each purified NK cell population was determined by flow cytometry, and the numbers of donor cells were adjusted accordingly, to ensure equal numbers of Ly49H⁺ NK cells of each genotype in the 1:1 mix. A total of 1.2×10^5 Ly49H⁺ NK cells in phosphate-buffered saline (PBS) was administered in recipient mice by intravenous (i.v.) injection one day before MCMV infection. For the non-competitive adoptive transfer assays, 1.2×10^5 Ly49H⁺ NK cells from a single mouse were injected.

In vivo MCMV infection and analyses of virus-specific NK cells

Stock salivary gland MCMV (Smith strain ATCC VR-1399, lot 1698918) was prepared as described.⁵⁸ Mice were infected with 7.5×10^2 plaque-forming units (pfu) of MCMV by intra-peritoneal (i.p.) injection one day after the NK cell transfer. Infection experiments were performed in a biosafety level 2 animal facility. To identify adaptive NK cells in blood or tissues, cells were isolated in the absence of infection or at the indicated times after infection, and Ly49H⁺ NK cells (NK1.1⁺ TCR β ⁻ Ly49H⁺) were identified by flow cytometry. Relative proportions and numbers of wild-type and mutant Ly49H⁺ NK cells were determined by staining for CD48 (which is expressed on all wild-type NK cells, but not SFR KO or CD48 KO NK cells) or CD45.1 (which is expressed on all wild-type NK cells, when wild-type SJL.B6 mice are used as donors, but not mutant NK cells). NK cell activation was monitored by detecting expression of CD69 and KLRG1, whereas proliferation was determined by analyzing expression of Ki67, using flow cytometry. Apoptosis and cell death were ascertained by assaying expression of activated caspases using flow cytometry. NK cell maturation was determined by examining expression of CD27 and CD11b.

Flow cytometry

Prior to staining cells with specific monoclonal antibodies (MAbs), cells were incubated for 30 minutes on ice with anti-CD16/32 (MAb 2.4G2) and mouse IgG2a (MAb 7G7; which blocks CD64) hybridoma supernatants, unless specified, to avoid non-specific staining due to binding of the Fc portion of MAbs to Fc receptors. After blocking, cells were stained with MAbs or the relevant isotype controls on ice for 30 minutes. Cells were then washed with PBS containing 2% fetal bovine serum (FBS) and analyzed. When cells were obtained from MCMV-infected mice, they were immediately fixed with the Fixation/Permeabilization Kit (BD Biosciences), to avoid MCMV contamination. For intracellular staining, cells were first permeabilized with the eBioscienceTM Foxp3/Transcription Factor Staining Buffer Set (ThermoFisher Scientific), as per the manufacturer's instructions. To detect activated caspases, cells were stained using the CaspGLOWTM Fluorescein Active Caspase Staining Kit (BioVision), as per the manufacturer's instructions. Fluorescence was monitored using a CyAnTM ADP Flow Cytometer (Beckman Coulter).

In vivo macrophage depletion

For macrophage depletion utilizing anti-colony-stimulating factor-1 receptor (CSF-1R) MAb, mice were injected IV with 400 μ g of anti-CSF-1R MAb (clone AFS98, Bio X Cell) or rat IgG2a isotype control (clone 2A3, Bio X Cell), three times a week for three weeks, prior to adoptive transfer of NK cells. To ensure maintenance of macrophage depletion, injections were continued three times a week after MCMV infection. For depletion experiments using clodronate, mice were injected i.v. with 200 μ l of clodronate liposomes or control liposomes (Liposoma) every three days, starting from 2 days prior to the adoptive transfer and until the end of the experiment.

With either approach, flow cytometry was conducted on day 7 to confirm macrophage depletion in spleen and monitor the abundance of donor NK cells in spleen or blood.

***In vitro* infection of macrophages with MCMV**

Recombinant MCMV-GFP virus was generated and titrated by the Dr. Ruzsics' group, as previously described.⁴¹ Mouse bone marrow-derived macrophages (BMDMs) were produced as described elsewhere.⁵⁹ In brief, femora and tibiae from 8-10 weeks old mice were flushed with PBS containing 2% FBS and propagated in bacterial Petri dishes for ~7 days, in complete DMEM supplemented with 30% (v/v) L929 cell-conditioned medium as a source CSF-1. At day 7, macrophages were harvested using cold PBS containing 2 mM-EDTA, and 5×10^4 cells were seeded overnight in a 24-well tissue culture plate in complete DMEM and 10% of L929 cell-conditioned medium. The next day, MCMV-GFP infection was performed using a multiplicity of infection (MOI) of 1:1 and centrifugal enhancement, as described.⁴¹ Cells were then incubated overnight at 37°C in a 5% CO₂ incubator and phagocytosis of NK cells was analyzed the next day.

Microscopy-based phagocytosis assay

To generate activated NK cells as targets, NK cells were activated with IL-15 (40 ng/ml), IL-12 (20 ng/ml) and IL-18 (10 ng/ml) in RPMI 1640 medium containing 10% FBS for 18 hours. They were subsequently labeled with Cell Trace Violet (CTV; 2.5 μM), for 10 minutes using the CellTrace™ Violet Cell Proliferation Kit (ThermoFisher Scientific). Then, NK cells were washed with PBS containing 2% FBS and centrifuged at 1500 rpm for 5 minutes. After incubating BMDMs in serum-free medium for 1h, 2×10^5 CTV-labelled NK cells were added to the BMDMs in the presence or not of 10 mg/ml of blocking anti-CD11a MAb (clone M17/4, eBioscience), blocking anti-CD18 MAb (clone GAME-46, BD Biosciences), rat IgG1 isotype control (clone R3-34, BD Biosciences) or rat IgG2a κ isotype control (clone eBR2a, eBioscience). When blocking MAbs were used in the phagocytosis assay, they were added to BMDMs 30 minutes before addition of NK cells. After incubation for 2 h at 37°C, BMDMs were extensively washed, and five images were taken for each condition using a ZOE Fluorescent Cell Imager (Bio-Rad) with the brightfield, blue and green acquisition channels. Images were merged, and phagocytosis was quantified by 2 different observers.

QUANTIFICATION AND STATISTICAL ANALYSIS

GraphPad Prism software (version 8) was used for unpaired or paired Student's t-tests (two-tailed), multiple t-test and one-way ANOVA followed by Tukey's multiple comparison tests, when appropriate. Statistical significance was determined by the probability (p) values, denoted by asterisks, which were set at ≤ 0.05 (*), ≤ 0.01 (**), and ≤ 0.001 (***), respectively. Any data that failed to reach statistical significance with p values greater than 0.05 were represented as "not significant" (ns). Unless specified, otherwise in the figure legends, the data are presented as mean \pm standard error of the mean (SEM). Figure legends provide information regarding the number of mice used to generate the data. This information was presented in the format "n = x", where "x" represents the number of mice. Throughout the project, about four blood samples were clotted after collection due to the large volume required to obtain enough Ly49H⁺ NK cells, making these samples unsuitable for analysis. Recollection of blood from these mice was not possible at the required time points due to ethical and animal welfare considerations. Therefore, these samples and their corresponding controls are not included in the results.

Cell Reports, Volume 43

Supplemental information

**Suppression of adaptive NK cell expansion
by macrophage-mediated phagocytosis
inhibited by 2B4-CD48**

Rui Li, Cristian Camilo Galindo, Dominique Davidson, Huaijian Guo, Ming-Chao Zhong, Jin Qian, Bin Li, Zsolt Ruzsics, Colleen M. Lau, Timothy E. O'Sullivan, Silvia M. Vidal, Joseph C. Sun, and André Veillette

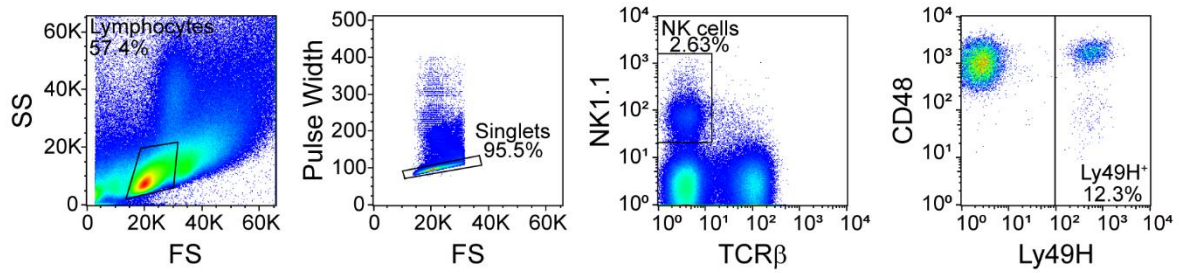
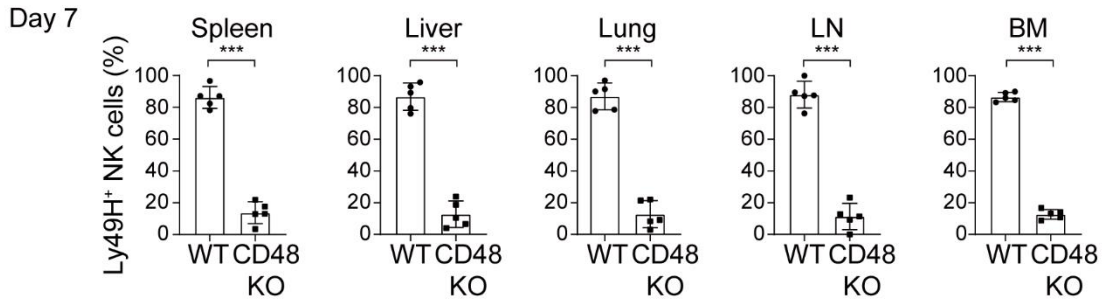
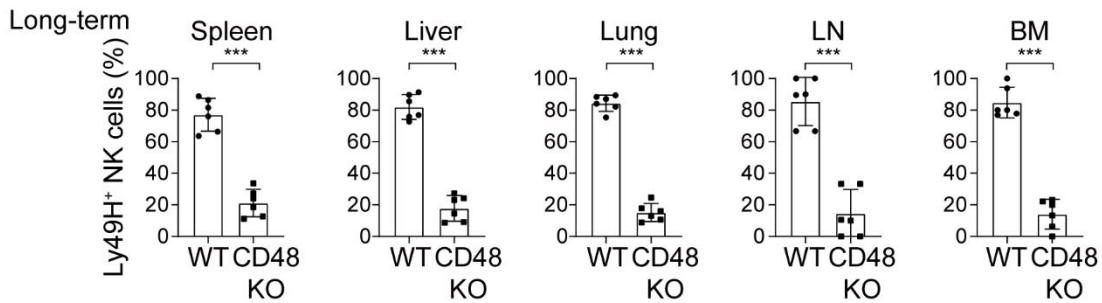
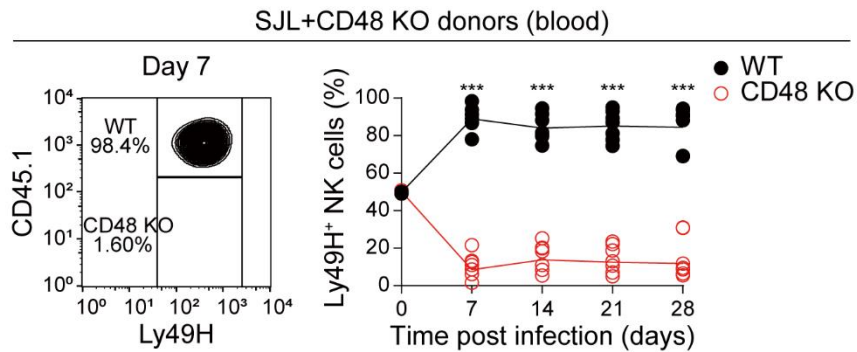
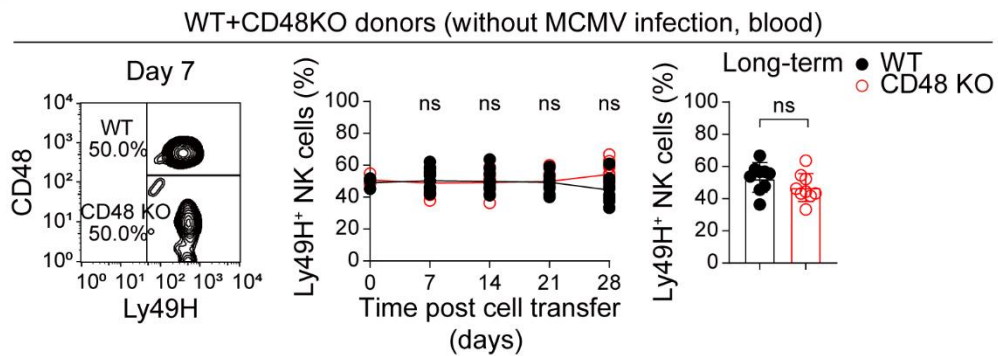
A**B****C****D****E**

Figure S1. CD48 deficiency selectively impairs MCMV-induced expansion of Ly49H⁺ NK cells. Related to Figure 1 and Figure 2.

(A) Representative flow cytometry analysis of the general gating strategy of Ly49H⁺ NK cells (NK1.1⁺, TCRβ⁻, Ly49H⁺) used in this study is depicted.

(B) Same as Figure 2B, except the proportions of WT and CD48 KO Ly49H⁺ NK cells were measured in various organs, including the spleen, liver, lung, lymph node (LN) and bone marrow (BM) at day 7 (n = 5).

(C) Same as (B), except the results on day 56 are depicted (n = 6).

(D) Blood. Equal numbers of Ly49H⁺ NK cells from WT(B6.SJL; CD45.1⁺/CD45.2⁻) and CD48 KO (CD45.1⁻/CD45.2⁺) donors were mixed and injected into Ly49H KO mice. The proportions of WT versus CD48 KO NK cells in the Ly49H⁺ population (NK1.1⁺, TCRβ⁻, Ly49H⁺) in blood of recipient mice were analyzed at indicated time points. CD45.1 was used as a marker to distinguish WT (CD45.1⁺) and CD48 KO (CD45.1⁻) cells. Left panel: representative flow cytometry analysis of CD45.1 expression on Ly49H⁺ NK cells at day 7. Proportions of WT (CD45.1⁺) and CD48 KO (CD45.1⁻) Ly49H⁺ NK cells are depicted. Right panel: proportions of WT and CD48 KO Ly49H⁺ NK cells at various time points in multiple independent mice (n = 7).

(E) Same as Figure 2B, except the adoptive transfer experiments were performed without MCMV infection. From left to right: first panel, representative flow cytometry analysis of CD48 expression on Ly49H⁺ NK cells in blood of recipient mice at day 7. Proportions of

WT (CD48⁺) and CD48 KO (CD48⁻) Ly49H⁺ NK cells are depicted. Second panel: proportions of WT and CD48 KO Ly49H⁺ NK cells at various time points in multiple independent mice (n = 9). Third panel: proportions of WT and CD48 KO Ly49H⁺ NK cells at day 35 in blood for multiple independent mice (n = 9).

Statistical analyses were conducted using unpaired t-tests (two-tailed), except in panels displaying data with multiple time points, where multiple t-tests were employed. Each symbol represents an individual mouse; error bars depict the mean with s.d. *p ≤ 0.05, **p ≤ 0.01, ***p ≤ 0.001, ns (not significant). Data are representative of 2 (B); 2 (C); 2 (D) and 3 (E) independent experiments, two to four recipient mice were injected with purified NK cells in each independent experiment.

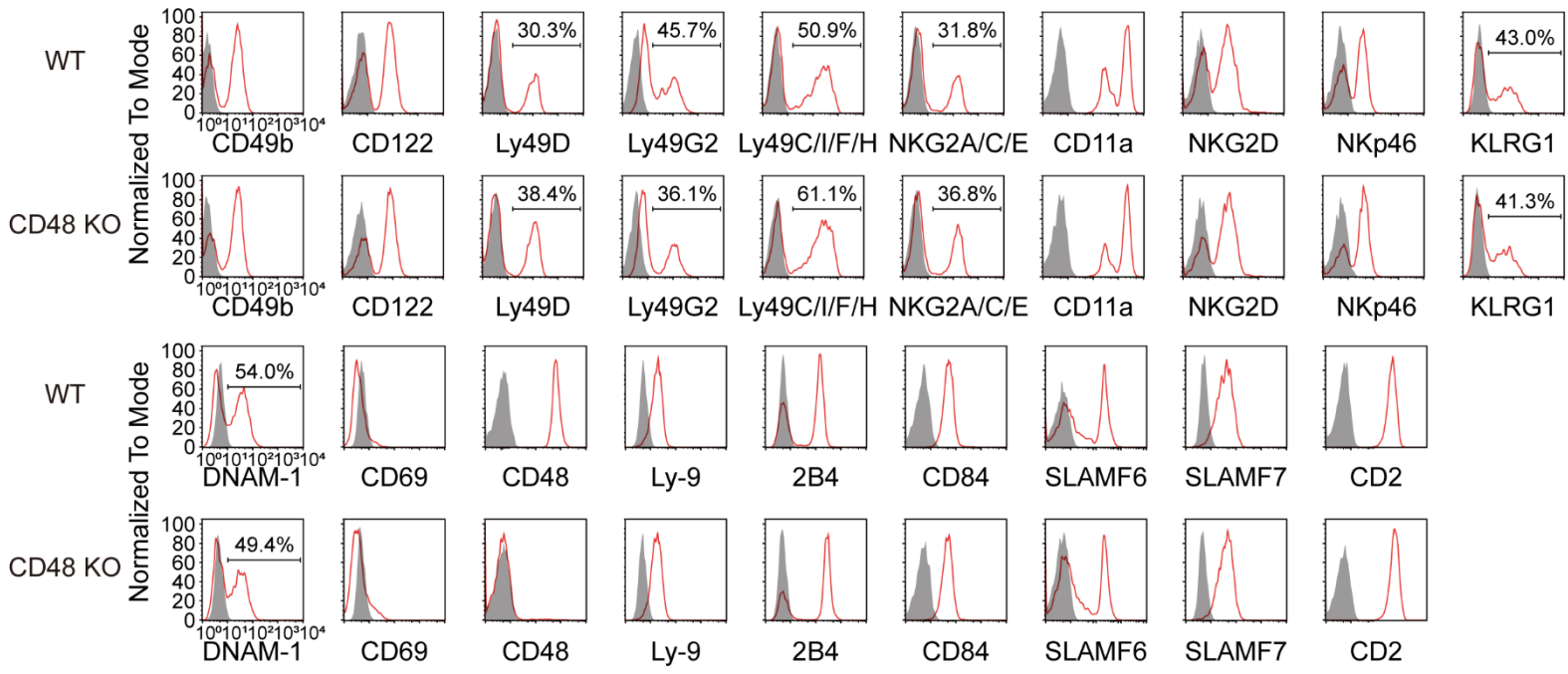
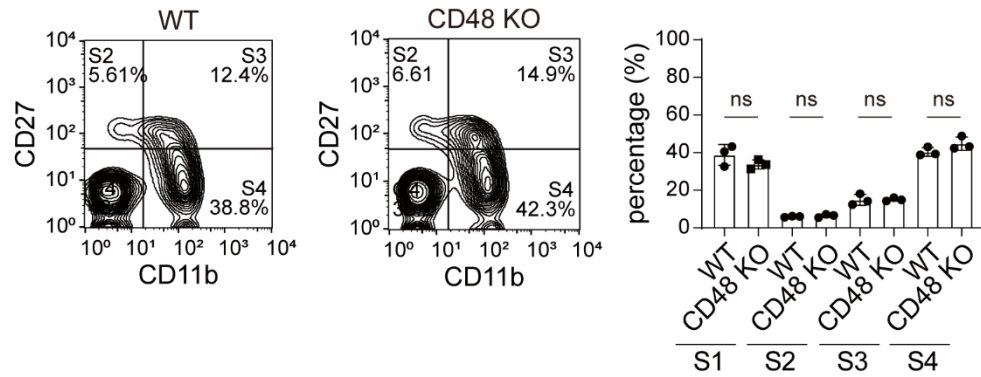
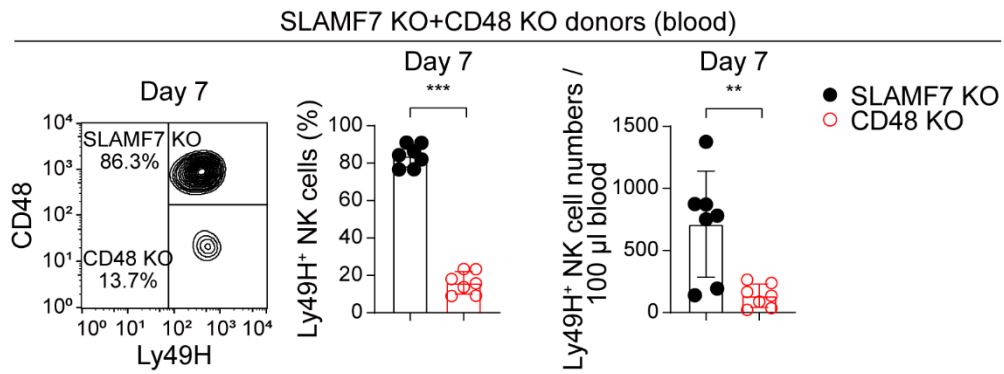
A**B****C**

Figure S2. CD48 deficiency does not affect NK cell development. Related to Figure 2.

(A) Representative flow cytometry analyses of NK cell receptor repertoires on freshly isolated splenic NK cells (NK1.1⁺, TCRβ⁻) from WT or CD48 KO mice (n = 3).

(B) Flow cytometry analyses of development of freshly isolated splenic NK cells (NK1.1⁺, TCRβ⁻) from WT or CD48 KO mice. CD11b and CD27 were stained to determine the development status of NK cells. Stage 1 (S1), CD11b⁻/CD27⁻; Stage 2 (S2), CD11b⁻/CD27⁺; Stage 3 (S3), CD11b⁺/CD27⁺; Stage 4 (S4), CD11b⁺/CD27⁻. From left to right: first two panels: representative analyses of CD11b and CD27 expression on WT and CD48 KO NK cells. Third panel: proportions of various developmental stages for WT and CD48 KO NK cells (n = 3).

(C) Equal numbers of Ly49H⁺ NK cells from SLAMF7 KO and CD48 KO donors were mixed and injected into Ly49H KO mice. The proportions of SLAMF7 KO versus CD48 KO NK cells in the Ly49H⁺ population (NK1.1⁺, TCRβ⁻, Ly49H⁺) in blood of recipient mice were analyzed at day 7. CD48 was used as a marker to distinguish SLAMF7 KO (CD48⁺) and CD48 KO (CD48⁻) cells. From left to right: first panel, representative flow cytometry analysis of CD48 expression on Ly49H⁺ NK cells at day 7. Proportions of SLAMF7 KO (CD48⁺) and CD48 KO (CD48⁻) Ly49H⁺ NK cells are depicted. Second panel: statistical analysis of the proportions for multiple independent mice (n = 7). Third panel: numbers of SLAMF7 KO and CD48 KO Ly49H⁺ NK cells per 100 μl blood (n = 7).

Statistical analyses were conducted using unpaired t-tests (two-tailed). Each symbol represents an individual mouse; error bars depict the mean with s.d. * $p \leq 0.05$, ** $p \leq 0.01$, *** $p \leq 0.001$, ns (not significant). Data are representative of 3 independent experiments.

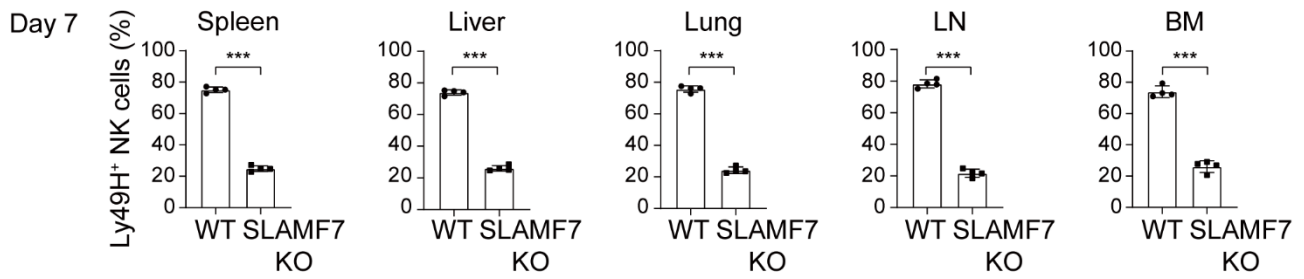
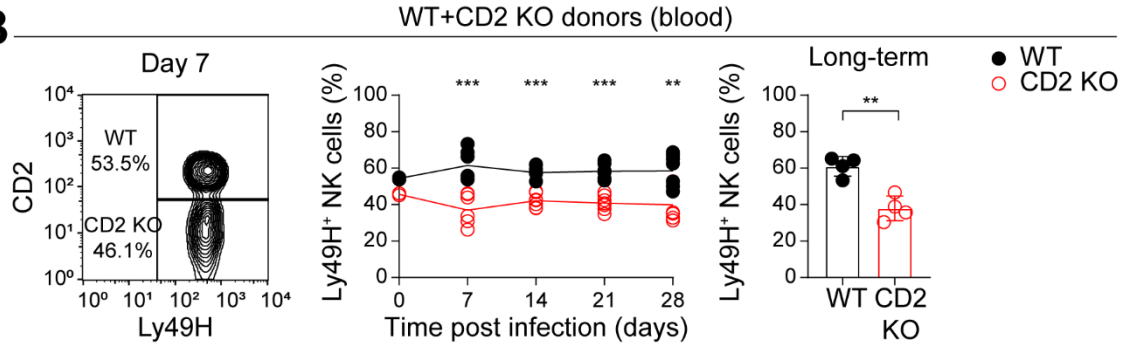
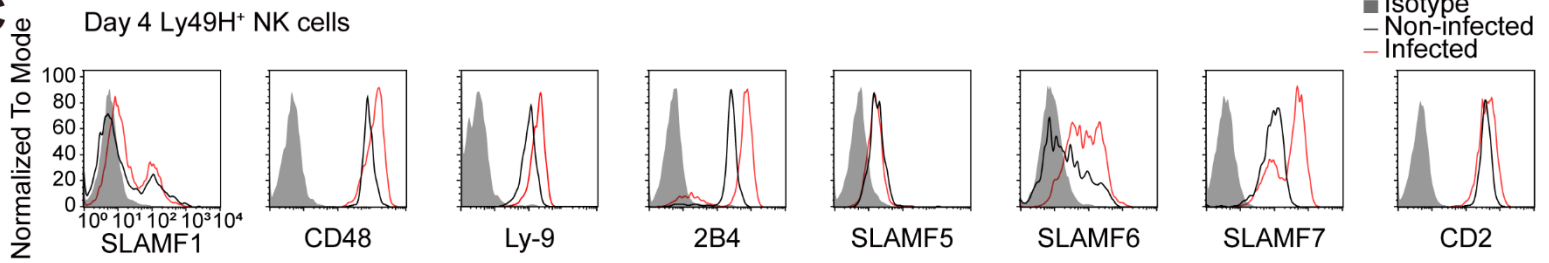
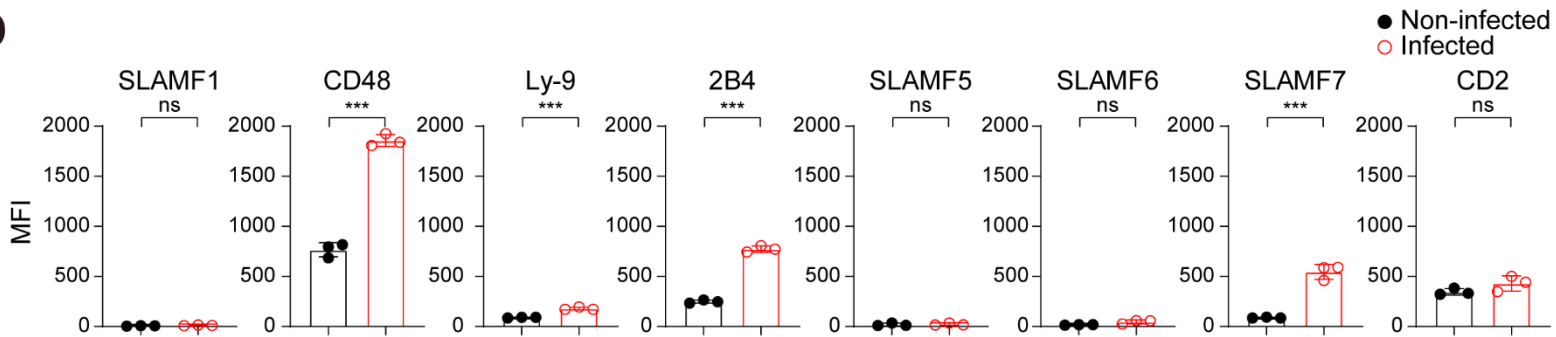
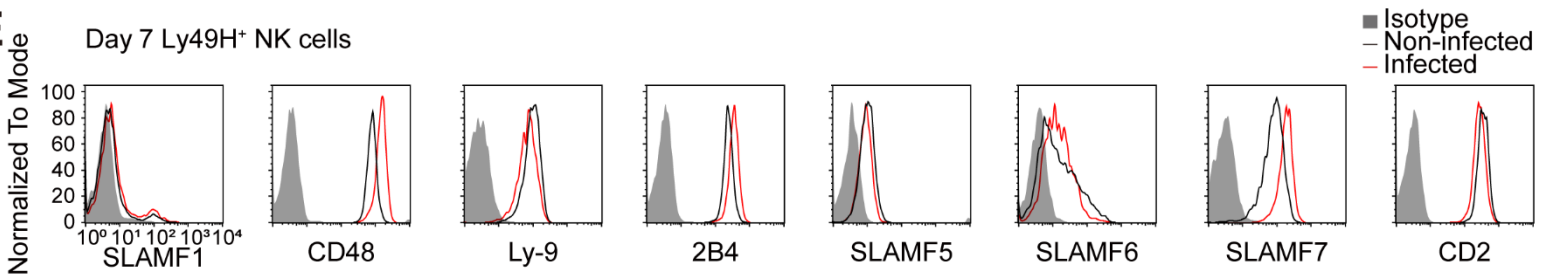
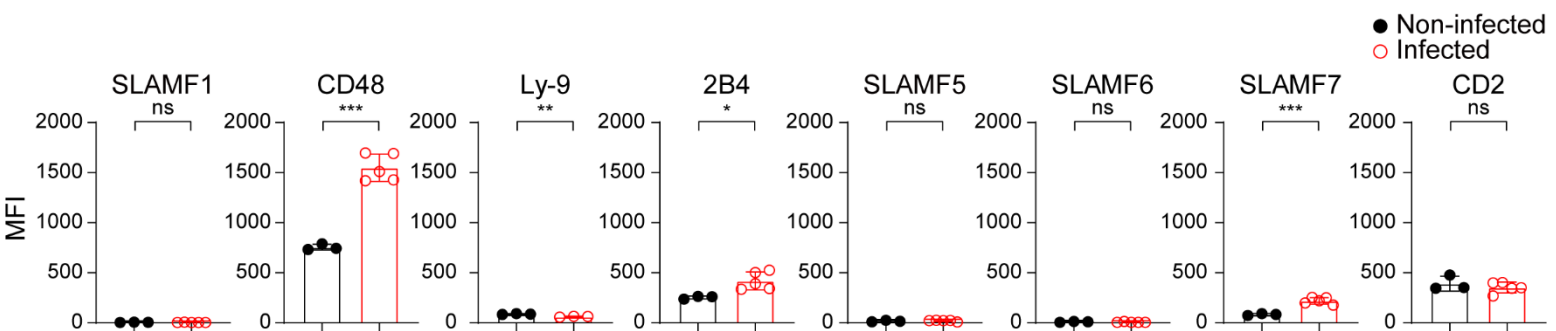
A**B****C****D****E****F**

Figure S3. CD48 plays a more crucial role than SLAMF7 in the expansion of Ly49H⁺ NK cells. Related to Figure 2.

(A) Same as Figure 2C, except the proportions of WT and SLAMF7 KO Ly49H⁺ NK cells were measured in various organs including the spleen, liver, lung, lymph node (LN) and bone marrow (BM) at day 7 (n = 4).

(B) Blood. Equal numbers of Ly49H⁺ NK cells from WT and CD2 KO donors were mixed and injected into Ly49H KO mice. The proportions of WT versus CD2 KO NK cells in the Ly49H⁺ population (NK1.1⁺, TCRβ⁻, Ly49H⁺) in blood of recipient mice were analyzed at indicated time points. CD2 was used as a marker to distinguish WT (CD2⁺) and CD2 KO (CD2⁻) cells. From left to right: first panel, representative flow cytometry analysis of CD2 expression on Ly49H⁺ NK cells at day 7. Proportions of WT (CD2⁺) and CD2 KO (CD2⁻) Ly49H⁺ NK cells are depicted. Second panel: proportions of WT and CD2 KO Ly49H⁺ NK cells at various time points in multiple independent mice (n = 6). Third panel: proportions of WT and CD2 KO Ly49H⁺ NK cells in blood at day 56 (n = 4).

(C) On day -1 (1 day before infection), Ly49H⁺ NK cells from WT donors were injected into Ly49H KO mice. On day 0, 7.5 x 10² pfu of MCMV were injected intra-peritoneally into recipients. The SLAM family receptors and CD2 expression on Ly49H⁺ NK cells (NK1.1⁺, TCRβ⁻, Ly49H⁺) in spleen of recipient mice were analyzed at day 4. Isotype controls are shown in grey, non-infected controls are shown in black, and the cells from

infected mice are shown in red. Representative flow cytometry analyses of the expression of the receptors on Ly49H⁺ donor NK cells at day 4 are depicted.

(D) Same as (C), except the statistical analyses of flow cytometry results for multiple mice are depicted (n = 3).

(E and F) Same as (C and D), except flow cytometry analysis results at day 7 are depicted. n = 3-5.

Statistical analyses were conducted using unpaired t-tests (two-tailed), except in panels displaying data with multiple time points, where multiple t-tests were employed. Each symbol represents an individual mouse; error bars depict the mean with s.d. *p ≤ 0.05, **p ≤ 0.01, ***p ≤ 0.001, ns (not significant). Data are representative of 2 (A); 2 (B) and 3 (C-F) independent experiments, one to four recipient mice were injected with purified NK cells in each independent experiment..

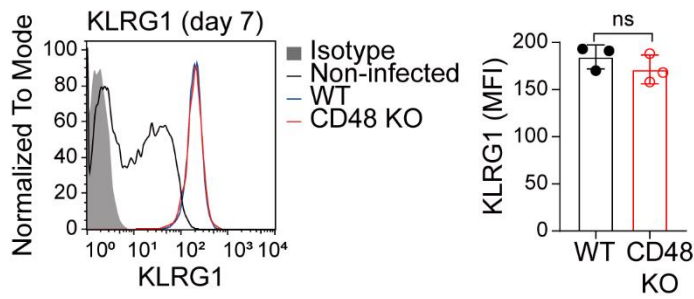
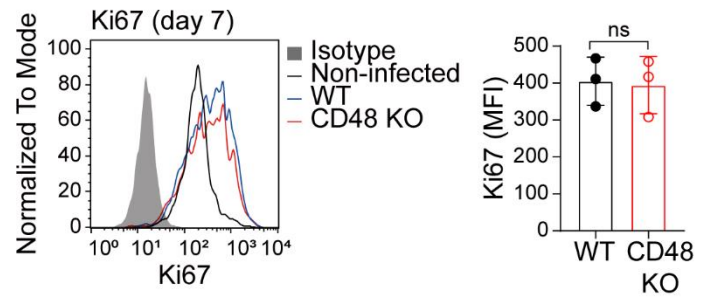
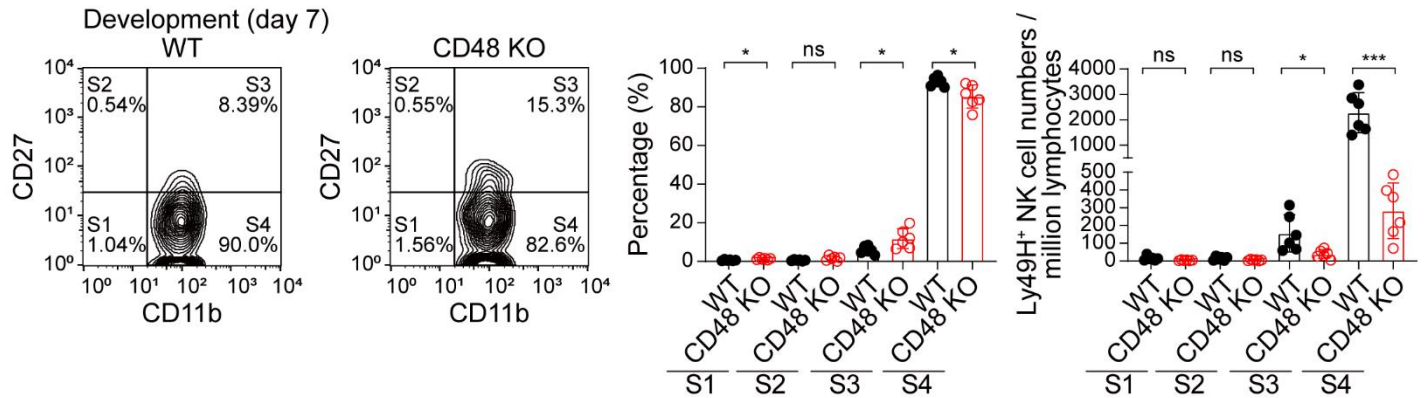
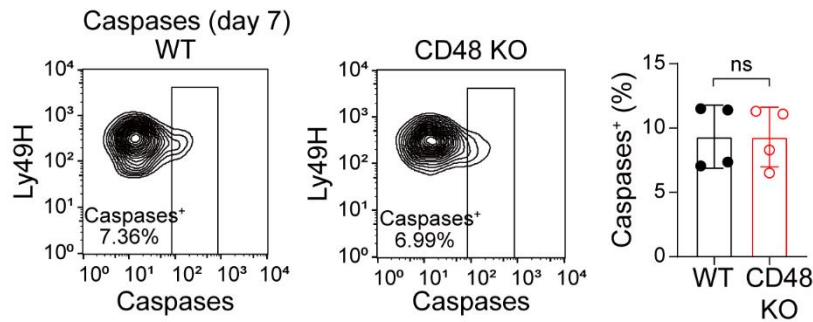
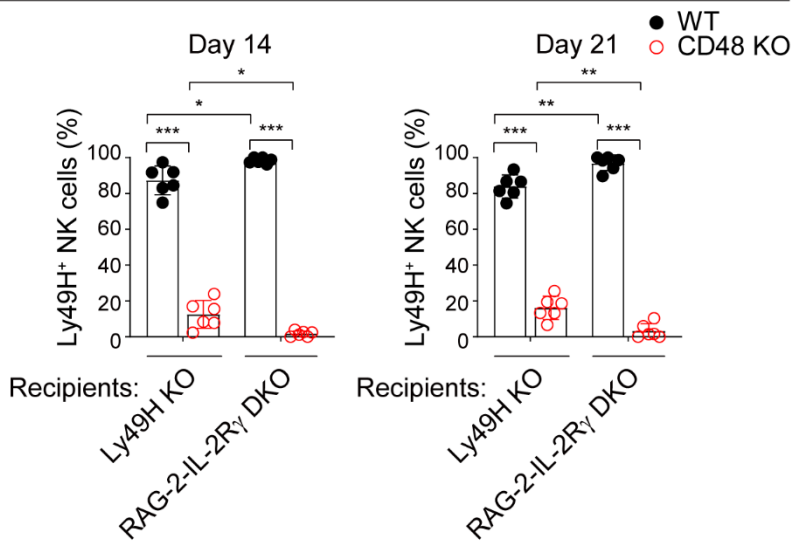
A**B****C****D**

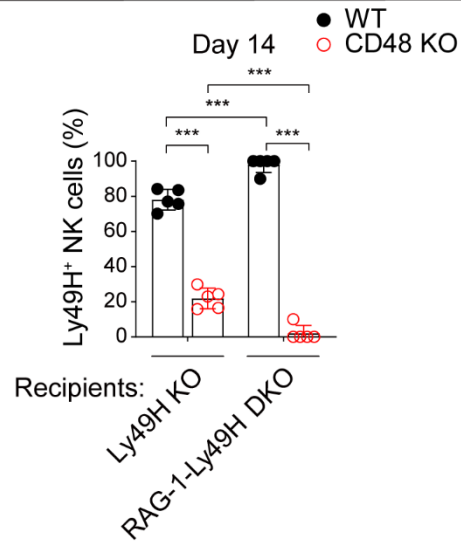
Figure S4. Minimal effect of CD48 deficiency on NK cell activation and proliferation.

Related to Figure 3.

(A-D) Same as in Figure 3B-E, except results at day 7 are depicted. Statistical analyses were conducted using unpaired t-tests (two-tailed). Each symbol represents an individual mouse; error bars depict the mean with s.d. * $p \leq 0.05$, ** $p \leq 0.01$, *** $p \leq 0.001$, ns (not significant).

AWT+CD48 KO donors; RAG-2-IL-2R γ DKO recipients (blood)**B**

WT+CD48 KO donors; RAG-1-Ly49H DKO recipients (blood)

**C**

WT+CD48 KO donors; RAG-1-Ly49H DKO recipients (blood)

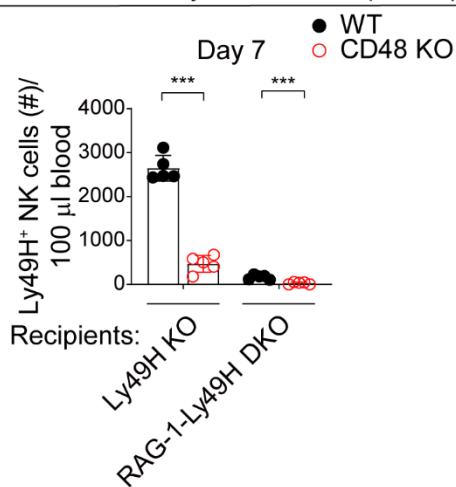
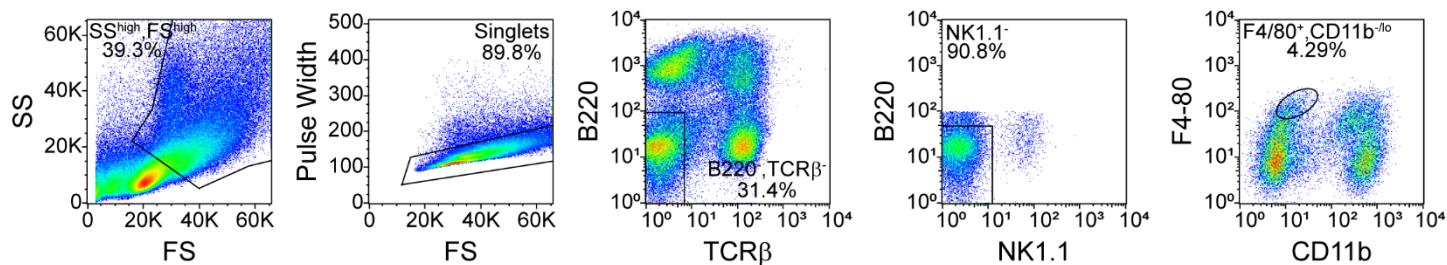
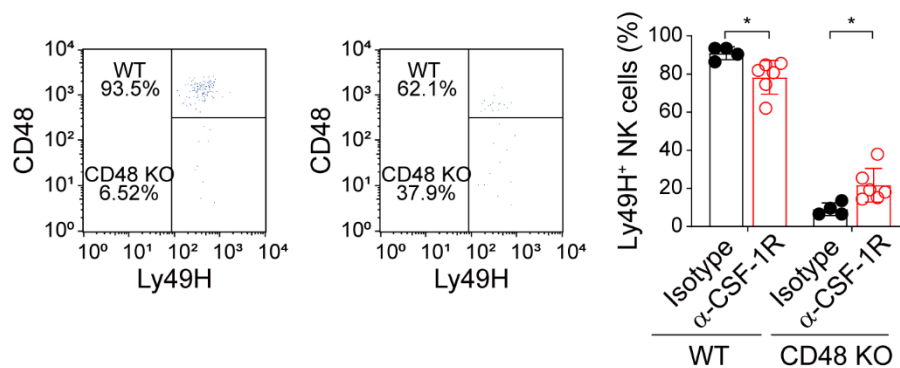
**D****E**Macrophage depletion (α -CSF-1R, blood)

Figure S5. Macrophages limit the expansion of Ly49H⁺ NK cells. Related to Figure 5.

(A) Same as in Figure 5B, except results at day 14 and day 21 are depicted (n = 6).

(B) Same as in Figure 5C, except results at day 14 are depicted (n = 5).

(C) Same as in Figure 5C, except numbers of WT and CD48 KO Ly49H⁺ NK cells per 100 μ l blood at day 7 are depicted (n = 5).

(D) Representative flow cytometry analysis of the general gating strategy of fresh isolated macrophages (B220⁻, TCR β ⁻, NK1.1⁻, F4/80⁺, CD11b^{-/lo}) used in this study is depicted.

(E) Same as Figure 5E, except blood was analyzed [n = 4 (isotype control); n = 6 (α -CSF-1R)].

Statistical analyses were conducted using unpaired t-tests (two-tailed), except in panels that involved comparisons of more than two groups, where one-way ANOVA followed by Tukey's multiple comparison tests were employed to assess significance. Each symbol represents an individual mouse; error bars depict the mean with s.d. *p \leq 0.05, **p \leq 0.01, ***p \leq 0.001, ns (not significant). Data are representative of 2 independent experiments, two to three recipient mice were injected with purified NK cells in each independent experiment.